

Observed tidal currents on the continental shelf off the east coast of India

A.K. Jithin^{1,2}, A.S. Unnikrishnan¹, Fernando Vijayan¹, M.P. Subeesh¹, R. Fernandes¹,
S. Khalap¹, S. Narayan¹, Y. Agarvadekar¹, M. Gaonkar¹, P. Tari¹, A. Kankonkar¹,
S. Vernekar¹

¹CSIR-National Institute of Oceanography, Dona Paula, Goa, India, 403004.

²Indian National Centre for Ocean Information Services, Ministry of Earth Sciences,
Hyderabad, India, 500090.

Corresponding Author: A.K. Jithin
Indian National Centre for Ocean Information Services,
Ministry of Earth Sciences, Hyderabad, India, 500090.
Email: jithinoceanography@gmail.com

Abstract

In the present study, we analysed 9-month long data from Acoustic Doppler Current Profilers (ADCP) deployed on the shelf off the east coast of India to study the characteristics of tidal currents in the region. The ADCPs were deployed at about 100-150 m depths off Cuddalore (CD, 12.0°N), Ramayapatnam (RM, 15.0°N), Kakinada (KN, 16.3°N) and South of Gopalpur (SG, 18.6°N). Tidal currents in the region are mainly semidiurnal in nature and dominant constituent is M₂. Semimajor axes of barotropic tidal ellipses of M₂ is about 1.9 cms⁻¹ in the southernmost ADCP location (off CD) and it is about 4.0 cms⁻¹ in the northernmost ADCP location (off SG), which indicate a northward increase of tidal currents. Baroclinic spectra shows high energy at tidal frequencies, which suggests the presence of internal tides on the shelf, particularly in the semidiurnal band. Semidiurnal internal tides of about 8-15 cms⁻¹ are observed at different locations and the magnitude is relatively large on the shelf off SG in the northern part of the shelf, which is primarily due to large barotropic forcing on the north. The semidiurnal internal tides are found to be intensified at the bottom, particularly on the shelf off SG and RM. The computed ratio of slope of internal wave characteristics (c) and topographic slope (γ) indicates that large near-critical regions present surrounding the ADCP locations off SG and RM could be the possible reason of bottom intensification at these two locations. EOF analysis shows that observed semidiurnal internal tides are dominated by the first baroclinic mode, where it accounts for about 70-80 % of semidiurnal internal tide variability on the shelf off SG and CD, whereas the contribution of the first mode is relatively small (43-50%) on the shelf off KN and RM. Enhanced small-scale vertical shear is observed on the ADCP locations associated with multimode structure of semidiurnal internal tides. Semidiurnal internal tides show a spring-neap variability on the shelf off SG and CD, whereas they are highly incoherent and intermittent on the shelf off RM and KN. Temporal variability of semidiurnal internal tide magnitude on the shelf is mainly due to the change in stratification, which is explained based on monthly climatology data.

Keywords: East coast of India, Continental shelf, ADCP, Internal tides, Bottom intensification, Tidal currents.

1. Introduction

It is observed that barotropic and internal tides (baroclinic tides) on the continental shelf and slope in various parts of the world ocean are strong to control various oceanic processes, such as vertical mixing and sediment transport. Besides, internal tides enhance biological productivity (Pingree et al., 1986). Barotropic tides in the ocean are generated by direct astronomical forcing, while the interaction of barotropic tidal currents with bottom topographic features such as continental shelves, slopes or ridges in a stratified ocean causes the generation of internal tides (Baines, 1982; Wunsch, 1975). As a result, a large part of global barotropic tidal energy gets converted to internal tides, hence internal tides act as a sink for global barotropic tidal energy (Egbert and Ray, 2000). Internal tides are internal gravity waves at tidal frequencies which can propagate to large distances from the generation region, for example, first mode internal tides can propagate thousands of kilometres without significant energy loss (Rainville and Pinkel, 2006). Generation and propagation of internal tides are influenced by bottom topography as well as background stratification. Internal tides on the continental margins propagate either in the onshore or in the offshore direction depending upon the slope of internal tide characteristics (c) and the slope of bottom topography (γ). Slope of internal wave characteristics is given by

$$c = \left(\frac{\omega^2 - f^2}{N^2 - \omega^2} \right)^{1/2} \quad (1)$$

Where ω and f are frequencies of internal tide and inertial oscillations respectively. N is the buoyancy frequency, calculated from vertical density gradient as

$$N^2 = - \frac{g}{\rho_0} \frac{\partial \rho}{\partial z} \quad (2)$$

Where ρ is the density and g is the acceleration due to gravity. ρ_0 is the reference density. The relationship between topographic slope (γ) and slope of internal wave characteristics (c) determines the generation and propagation of internal tides on the continental shelf and slope. (i) If the region is critical ($\gamma=c$), the generation of internal tides generally occurs. (ii) If $\gamma < c$ (subcritical), internal waves propagate towards the coast. (iii) If $\gamma > c$ (supercritical), internal waves reflect back to the offshore direction (Baines, 1982).

Studies on tides in the Bay of Bengal (BoB, Fig. 1) are limited and drew more attention in the recent years. Tides in the Bay are predominantly semidiurnal in nature and the amplitude of major semidiurnal constituents increases towards the head of the bay (Table. 1). Murty and Henry (1983) developed a numerical model for the propagation of tides in the BoB. They described tidal

characteristics in the BoB based on co-tidal and co-range charts for the major tidal constituents (M_2 , S_2 , K_1 and O_1) from the model simulations. Sindhu and Unnikrishnan (2013) used a two-dimensional vertically integrated numerical model using modified shelf bathymetry data to simulate tides in the BoB. Their study discussed the characteristics of tidal propagation throughout the Bay using co-tidal and co-range charts for major tidal constituents and found that the amplitudes of semidiurnal tide amplify nearly twice at the head of the bay and in the Gulf of Martaban due to wide continental shelf. Maximum amplitude of M_2 (180 cm) and S_2 (80 cm) tide is observed in the Gulf of Martaban and maximum amplitude of diurnal constituent, K_1 (about 20 cm) is observed in the Malacca Strait.

Though characteristics of tides in the BoB are known relatively well, the understanding of tidal currents in the coastal regions in the Bay is poor and only a few studies are found in the literature. A few studies using 2D models have reported on the magnitudes of tidal currents in the coastal regions off the east coast of India. For instance, Misra et al. (2011) reported that tide-induced currents have magnitude of about 12 cms^{-1} in the near shore region off Chennai (about 13° N). Similarly, Misra et al. (2013) simulated tide-induced currents off the east coast of India reported that magnitude of tidal currents at 20 m depth increases from Nagapattinam (about 11.7° N) to Paradip (about 20.3° N) from about 7.5 cms^{-1} to 24.9 cms^{-1} respectively. Apart from the barotropic tidal currents, presence of internal tides was reported in some earlier studies. One study, which goes back to the 1950's, carried out by Lafond et al. (1954) using bathythermograph data collected off the central east coast of India, reported vertical oscillations in the temperature fields at tidal periods. Studies using short-period records of temperature and current observations reported oscillations at semidiurnal periods in some regions, such as, off Godavari estuary along the east coast of India (Sarma and Rao, 1989), upper layers off west of Andaman Islands (Sarma et al., 1991) and in the central BoB (Kumar et al., 2001). Using space borne Synthetic Aperture Radar (SAR) imageries, Prasad and Rajasekhar (2010) reported the presence of shoreward propagating short-period internal waves in all seasons on the continental shelf off Chilika (19.71° N), northern BoB. Temperature data collected off Bhimilipatanam (about 17.9° N) show large internal wave oscillations in bottom levels (54-95 m) at tidal periods (Sridevi et al., 2010). Similarly, temperature data collected off Gopalpur (Fig. 1) show that internal waves at tidal periods in the bottom levels (50-100 m) are stronger than those at the surface (Pradhan et al., 2013). Numerical simulations and observations of internal waves along the east coast of India indicate that internal wave activity is predominantly observed on the northern part of the shelf ($17-22^\circ \text{ N}$) and maximum internal wave activity occurs in semidiurnal frequencies generated on the slope or shelf-break regions by tidal flow (Pradhan et al., 2013; Rao et al., 2010, 2011;). All these studies are based on numerical modelling or limited to the analysis of

short-period observations. In the present study, we report a detailed analysis of barotropic and internal tides using long-term Acoustic Doppler Current Profiler (ADCP) measurements at different locations on the continental shelf off the east coast of India (Fig. 1).

Spatial and temporal variability of stratification could alter the internal tide field on the continental shelf, especially in those regions exhibiting large variability in seasonal and synoptic scale (Bravo et al., 2013). The north Indian Ocean experiences Southwest (SW) monsoon season during June to September and Northeast (NE) monsoon during November to January. Various studies based on hydrographic measurements in the region suggest that density stratification is highly modified by monsoonal winds, seasonally reversing coastal current and large freshwater input from the adjacent rivers (Kumar et al., 2013; Shetye et al., 1991, 1996). Shetye et al. (1991) observed an upwelling band approximately 40 km wide off the east coast of India during the SW monsoon. This results in a shoreward increase of salinity and a weak vertical stratification near to the coastal regions during SW monsoon. The Bay receives large amounts of freshwater from the continental rivers during the SW monsoon (Chaitanya et al., 2014; Papa et al., 2012). This fresh water discharge increases the near-surface stratification on the northern part of the shelf during September-October months and it gradually gets advected towards the south along the coast. During NE monsoon, this fresh water plume is observed along the entire east coast. The buoyancy frequencies computed at the ADCP mooring locations from the revised climatology of temperature and salinity (Chatterjee et al., 2012), show large variations from SW monsoon to NE monsoon seasons (Fig. 2). Apart from the seasonal variations, stratification and physical characteristics can vary across the shelf and slope due to the presence of frontal systems and mesoscale eddies. For example, Kumar et al. (2013) observed coastal thermohaline fronts off the central east coast of India (about 17.92°N) during NE monsoon, having strong vertical and lateral density gradients between the shelf and slope. These frontal systems are generated by the southward advection of low salinity water from the northern BoB and mesoscale re-circulation around an eddy. In brief, stratification along the coast varies considerably in seasonal and intra seasonal time scales and it could lead to changes in internal tide field.

Long-period observations of currents with high temporal resolution are useful for the study of characteristics of tidal currents. Measurements using ADCPs deployed on the continental shelf and slope at about 100 m and 1000 m depths respectively off the east coast of India provided a unique opportunity to study tidal currents in the region (Fig. 1). In an earlier study, these ADCP observations were used to study intra-seasonal variability of the East India Coastal Current (EICC) and near-inertial currents (Mukherjee et al., 2013, 2014). Similarly, ADCP measurements on the

shelf and slope off the west coast India were used for the study of tidal currents (Subeesh et al., 2013; Subeesh and Unnikrishnan, 2016). They observed strong tidal currents on the northern part of the shelf, for instance, the cross-isobath velocity of barotropic tidal currents reach up to about 32 cm s^{-1} on the shelf off Mumbai (20.0°N) in the north. The magnitude of internal tides ranges between $10\text{-}20 \text{ cm s}^{-1}$ on the shelf off the west coast of India and an increase of internal tides was observed during pre-monsoon to SW monsoon period due to the increases in the background stratification on the shelf. The main objective of the present study is to describe the characteristic features of barotropic and internal tides on the continental shelf off the east coast of India. We also try to examine the seasonal variations in internal tides. The paper is organised as follows. A description of ADCP data and the analysis of tidal currents is given in Section 2. Results are described in Section 3 followed by Discussions and Conclusions in Section 4.

2. Data and Methods

A series of RDI ADCPs were deployed along the continental shelf and slope off the east coast of India as part of EEZ mooring programme started in 2009 by the CSIR-National Institute of Oceanography. The ADCPs were deployed on the shelf off Cuddalore (12.01°N , hereafter CD), Ramapatnam (15.00°N , hereafter RM), Kakinada (16.30°N , hereafter KN) and south of Gopalpur (18.64°N , hereafter SG) at 150 m, 100 m, 120 m and 97 m depths respectively (Fig. 1). ADCPs were also deployed on the continental slope region off these locations at depths of about 1000m. In the present study, we focus the discussion on the analysis of data from the shelf. Continental shelf is narrow along the east coast of India with widths varying from about 30 km to 60km at KN and RM respectively (Table 2). ADCP moorings on the shelf off CD and KN are located near the shelf edge. All moorings were equipped with a bottom-mounted upward looking 300 kHz ADCP recording data at every 15 or 30 minutes. All ADCP moorings on the shelf have data coverage of more than 77% of the water column. Details are provided in Table 2. Quality of current data at all locations was checked carefully and spurious peaks were removed. Current data at the surface ($<10 \text{ m}$) and in the bottom layers (about $5\text{-}10 \text{ m}$) were removed due to the possibilities of data contamination. After the quality check, the study period of our analysis was restricted to 9-month (June-February) period covering various years (Table 2). The data were grouped into four two-month subsections, those of July-August and November-December, which represent the SW and NE monsoon respectively and, September-October period is considered as the transition period between the SW and NE monsoons. January to February period is considered as late NE monsoon. Barotropic and baroclinic tidal currents calculated at all locations were used to describe their spatial and temporal variability.

Barotropic currents were calculated by average in raw currents in the vertical and baroclinic currents were determined by subtracting the barotropic current from raw current. Baroclinic currents were rotated with respect to the local bathymetry for obtaining cross-isobath as well as along-isobath components of the current and angle of rotation at each location is shown in Table 2. Barotropic and baroclinic tidal constituents were computed by harmonic analysis with error estimates using `t_tide` tool (Pawlowicz et al., 2002, <http://www.ocgy.ubc.ca/~rich>). Semidiurnal constituents (M_2 and S_2) are found to be significant in these regions, whereas diurnal constituents (K_1 and O_1) are relatively small. Tidal ellipses were prepared for M_2 and S_2 for both barotropic and baroclinic tidal currents. We also determined baroclinic tidal currents for the semidiurnal period using third order Butterworth band-pass filter for 10-14 hours. Vertical modes of internal tides were determined using Complex Empirical Orthogonal Function (CEOF) analysis.

There are no temperature and salinity data available at the mooring sites during the study period. Hence, available CTD observations near to the ADCP moorings collected during other years (period is shown in Fig. 10) and temperature and salinity from revised climatology of the North Indian Ocean (Chatterjee et al., 2012) were used to analyse the seasonal variation of vertical stratification and compute buoyancy frequency near the mooring site. Large buoyancy frequencies and large vertical density gradient indicate that water column is highly stratified during NE monsoon period at the ADCP locations on the southern part of the shelf, while water column is highly stratified during September to October period in the northern part (Fig. 2). Bathymetric slope near to the ADCP moorings was calculated using high resolution bathymetry data (SRTM30_PLUS http://topex.ucsd.edu/WWW_html/srtm30_plus.html) and slope of M_2 internal tide characteristics was computed using bottom buoyancy frequency computed from climatology.

3. Results

3.1 Barotropic tidal currents on the shelf

Vertically-averaged raw currents for the 9-month period were subjected to harmonic analysis to determine the amplitudes and phases of various tidal constituents. The largest tidal constituent in the region is M_2 followed by S_2 , which is consistent with the semidiurnal nature of tides in the BoB reported in earlier studies (Murty and Henry, 1983; Sindhu and Unnikrishnan, 2013). Tidal ellipse parameters of M_2 and S_2 were calculated from the amplitude and phase of both eastward and northward velocity components for all locations on the shelf (Table 3). Maximum value of semi major axis of M_2 is observed on the shelf off SG (3.98 cms^{-1}) in the north and minimum is found on the shelf off CD (1.87 cms^{-1}) in the south. There is a gradual increase of M_2 tidal currents towards the

northern part of the shelf (Table 3). S_2 is the second largest tidal constituent and maximum amplitude is observed on the shelf off SG (1.9 cms^{-1}). Amplitude of N_2 is one-third that of M_2 on the shelf off SG (1.3 cms^{-1}) and KN (1.1 cms^{-1}) whereas it is very small (about 0.6 cms^{-1}) and roughly one-fourth of M_2 off CD and RM. Amplitude of diurnal tidal constituents (K_1 and O_1) on the shelf are the order of about $0.5\text{-}1 \text{ cms}^{-1}$. Tidal constituents with the amplitude less than 1 cms^{-1} (O_1 , K_1 and N_2) were not considered in further discussion.

M_2 tidal currents rotate in an anticlockwise direction on the shelf off CD and KN, whereas the rotation is in the clockwise direction on the shelf off RM and SG. The latter is expected for the ellipses in the northern hemisphere. Barotropic M_2 and S_2 ellipses are oriented nearly in a cross-isobath direction on the shelf off CD, RM and SG (Fig. 3). However, tidal ellipses of M_2 and S_2 are nearly rectilinear and oriented quasi-parallel to the isobath on the shelf off KN, which indicates that semidiurnal tidal currents flow nearly parallel to the coast in the region. Co-tidal charts show that M_2 tide in the bay propagates from the south to north (Sindhu and Unnikrishnan, 2013). Northward propagating tides in the bay could be oriented towards northeast due to the orientation of the coast north of RM and tidal currents tend to flow in the alongshore direction off KN.

We used TPXO7.2 tidal model results (extracted using Oregon State University Tidal Prediction Software, hereafter OTPS), extracted at points close to the mooring locations, for comparison with computed barotropic currents from ADCP. The tidal elevations computed from the pressure variations recorded by the pressure sensor in the ADCP are in phase with the tidal elevation predicted by TPXO7.2 tidal model (figure not shown). Current observations in the region are scarce and it is useful to know accuracies of simulated tidal currents from a global tidal model on the shelf off the east coast of India. A comparison of tidal currents from ADCP observation and TPXO7.2 model simulations show that both are in phase, but the latter underestimates the magnitudes (Fig. 4).

3.2 Current Spectra

Rotary spectra were computed using the baroclinic currents to study the energy distribution at various frequencies (Fig. 5). Depth-averaged clockwise (CW) and counter clockwise (CCW) components of rotary spectra show large spectral energy in the semidiurnal band (M_2 and S_2) compared to those in diurnal frequencies (K_1 and O_1). Spectral energy of CW component is larger than over CCW component in all frequencies. Theoretically, the dominance of CW component over CCW component (ratio of CC and CCW is greater than 1) is expected in the northern hemisphere (Gill, 1982). Small spectral peaks at near-inertial frequencies indicate that near-inertial waves are weak on the shelf. Mukherjee et al. (2013) reported that near-inertial currents on the shelf are found

to be weak compared to those on the slope, because of the small width of the continental shelf compared to the Rossby radius of deformation in the region. Predominance of spectral energy at tidal frequencies, particularly in the semidiurnal band suggests that the internal wave motions in the region are mostly confined to semidiurnal internal tides. Spectral peaks at diurnal frequencies are found to be narrow, while spectral energy is distributed in a wide spectral band at semidiurnal frequencies. Further, significant spectral peaks at higher order harmonics (M_4 , M_6 and M_8) suggest the presence of non-linearity (Fig. 5). Relatively large semidiurnal baroclinic energy is found on the shelf off SG in the northern part of the shelf where it accounts for about 45% of the total energy in the internal wave band (f to N). For the other locations CD and KN, it is about 29% and for RM, it is about 18%. Since most part of the energy for the baroclinic tides is confined to semidiurnal frequencies in the spectra, our present study mainly concentrated on the analysis of semidiurnal internal tides and their characteristics.

3.3 Internal tides on the shelf

3.3.1 Baroclinic M_2 tidal ellipses

Among the semidiurnal constituents, M_2 has the largest amplitudes followed by S_2 . We focus our discussion on the characteristics of M_2 internal tides using baroclinic ellipses. Baroclinic M_2 tidal ellipses determined for two-month periods (July-Aug, September-October, November-December and January-February) were used to study their vertical structure and seasonal variability on the shelf (Fig. 6). Among the four locations, largest M_2 ellipses are observed on the shelf off SG in the north followed by CD and relatively small ellipses are found off RM and KN. Strong barotropic forcing in the cross-isobath direction is primarily responsible for strong internal tides off SG. Off KN, the barotropic ellipses are aligned in an along-isobath direction, thereby cross-isobath component is not strong to generate internal tides having similar magnitudes those off SG (Fig. 3). Baroclinic M_2 ellipses are nearly oriented in a cross-isobath (along-isobath) direction on the shelf off RM and SG (off CD and KN). In vertical, minimum amplitude of baroclinic ellipses is observed at the mid-depths at all the locations. Large amplitude of M_2 internal tides near the bottom and surface layers with mid-depth minima generally indicates a first mode structure. The vertical structure of M_2 ellipses is more complex on the shelf off KN and RM compared to other locations. Maximum values of semimajor axes of M_2 ellipses are observed at the bottom levels indicating bottom intensification of M_2 internal tides, particularly on the shelf off SG during all the seasons (Fig. 6d) whereas intensification of M_2 internal tides is not a permanent feature in the other locations (off RM).

M_2 ellipses rotate mostly in the clockwise direction on the shelf off CD and SG, which is

consistent with the linear theory of internal waves (Gill, 1982). Both clockwise and anticlockwise rotation of M_2 internal tides are observed off RM and KN and the sense of rotation varies with depth (Fig 6). Sudden change of phase of M_2 internal tides between different vertical levels is observed near to the depth of minimum amplitude (Fig. 6). Phase of M_2 internal tides in different vertical levels do not show a continuous change with depth. However, approximately 180° phase difference is found between the upper and lower levels of the water column. For example, M_2 internal tides show nearly 180° phase lag between surface and bottom levels on the shelf off RM and SG during SW monsoon (Fig. 6b and d).

Baroclinic ellipses show that magnitude of M_2 internal tides varies with seasons. Strong M_2 internal tides with semi-major axis about $7-13 \text{ cms}^{-1}$ are observed near the surface (13-25 m) and bottom levels (70-85m) on the shelf off SG during SW monsoon, transition months and late NE monsoon period, whereas they become weakened ($3-7 \text{ cms}^{-1}$) during NE monsoon season (Fig. 6d). M_2 internal tides off RM are weak ($1-3 \text{ cms}^{-1}$) but amplitudes becomes $3-6 \text{ cms}^{-1}$ during NE monsoon season. Similarly, strong M_2 internal tides are observed during NE and late NE monsoon seasons off CD. In the southern mooring locations (off CD and RM), large M_2 ellipses are observed during NE monsoon, whereas large M_2 ellipses are observed on the shelf off KN during SW monsoon and off SG during the transition months (September-October). Buoyancy frequency computed using the climatological values of temperature and salinity shows that the observed variations in the magnitude of M_2 internal tides have a strong dependency with stratification (Fig. 6 and Fig.2). Large baroclinic M_2 ellipses are observed during the transition period (NE monsoon) when the stratification is strong on the shelf off SG (CD). Seasonal variability of stratification can alter the internal tide field on the shelf and this has been reported in many earlier studies (for instance, Bravo et al., 2013; Subeesh et al., 2016; Guo et al., 2012). However, there are instances where the internal tide variability that could not fully explained by climatological stratification alone. Further discussions on the spatial and temporal variability of internal tides considering barotropic forcing, topography and stratification are given in Section 3.3.4.

We also determined baroclinic tidal ellipse parameters for S_2 and N_2 on the shelf (Appendix A). Maximum value of semimajor axis (8.4 cms^{-1}) of S_2 is observed on the shelf off SG during September-October period and the vertical structure and seasonal variability of S_2 are similar to those of M_2 internal tides. N_2 internal tides are smaller than those of S_2 and the maximum value of semimajor axis of N_2 ellipse reaches up to 5.4 cms^{-1} on the shelf off SG. Bottom intensification is also observed for S_2 and N_2 internal tides off SG.

3.3.2. Band-passed semidiurnal internal tides

Time series of semidiurnal band-passed (10-14 hour period) baroclinic tidal currents at different levels are shown in Fig.7. Tidal elevations from TPXO7.2 model simulations were extracted at the closest grid point of the mooring site are also shown in Fig. 7. Band-passed diurnal internal tides, computed for 22-26 hours are found to be small on the shelf ($2-4 \text{ cms}^{-1}$) and they were not considered in the present analysis. Semidiurnal internal tides at the ADCP locations on the shelf are typically of the order of $8-15 \text{ cms}^{-1}$ (Fig. 7). Relatively strong semidiurnal internal tides (about 15 cms^{-1} at 75-85m depth) are observed on the shelf off SG in the north, where they are about 20% of the total baroclinic currents. Along-isobath component of semidiurnal internal tides is strong on the shelf off CD and KN, whereas cross-isobath component is strong on the shelf off RM and SG. This indicates that semidiurnal internal tides are found to be strong in the direction of barotropic ellipses on the shelf off RM, KN and SG, except on the shelf off CD (Fig. 3 and Fig. 6). Semidiurnal internal tides on the shelves off CD and SG, show a spring-neap variability (period of 14.79 days) similar to those of barotropic tides. In the other two locations (RM and KN), semidiurnal internal tides are found to be intermittent and spring-neap variability is nearly absent. This is due to the presence of incoherent internal tides in these regions.

3.3.3. Coherent and Incoherent internal tides on the shelf

Coherent internal tides are defined as the time independent part of internal tide phase-locked with surface tide, which retain its amplitude and phase for a given period of time (Nash et al., 2012). This can be largely explained by background stratification and surface forcing. The incoherent internal tide is a time-variable part uncorrelated with surface tide, which arises due to changes in background stratification, shoaling, modulation by background currents and mesoscale eddies (Rainville and Pinkel, 2006; Kelly and Nash, 2010; Ponte and Klein, 2014). Coherent internal tide can be calculated from the harmonic analysis of sufficiently long time-series, which separate out the phase and amplitude retains for the given period of time. We used 9-month long time series to conduct harmonic analysis. First the broadband (10-14 hour) semidiurnal internal tide signal was extracted using third order Butterworth filter. Harmonic analysis was carried out on the broadband signal and coherent part was separated out. M_2 , S_2 , S_2 and L_2 constituents were retained in the control file and all other constituents were removed. Rest of the signal which is the deviation of band passed signal from the coherent part, is considered as the time-variable incoherent. We found that full period (9-month) harmonic analysis captures only about 2-8% of variance (Table 4).

We also did running harmonic analysis for different time spans to estimate the capability of

harmonic analysis to represent internal tides in different time windows (length of the data used for the analysis), following the approach by Nash et al (2012). The harmonic analysis was carried out for different time windows varying from 3 days to 9 months and the results are presented in Table 4. Fig. 8 shows the results from 30-day running harmonic analysis (Here, variance computed from harmonic analysis result is considered as coherent). On the shelf off SG, 30-day running harmonic analysis captures about 64% of the variance, which is relatively large compared to those obtained for the other locations on the shelf such as CD, RM and RN, where it captures 45%, 35 % and 28% respectively (Table 4). This indicates that percentage of variance explained by 30-day running harmonic analysis is less than 50% of total semidiurnal band in most of the locations on the shelf. Variance computed from 30-day running harmonic analysis shows spring-neap and seasonal modulations on the shelf off CD and SG (Fig. 8). Further, percentage of variance captured by harmonic analysis is found to decrease, for the results obtained for large time windows. The percentage of variance obtained from 3-day running harmonic analysis explains about 91-95 % of variance of the total semidiurnal band which gets reduced to about 17-37% in a 60-day window at all the locations. Percentage of variance decreases drastically from 3 to 15-day window off RM and KN, whereas significant decrease in the percentage is observed off CD and SG in large time windows (15-60 day). Differences found in the two time windows indicate that internal tide variability occurs at multiple time scales in different locations on the shelf. Nash et al (2012) studied the predictability of internal tides using harmonic analysis on the shelf by considering different shelf locations around the world oceans and showed that internal tides are largely unpredictable in nature. Similar to other locations around the world, for instance, Mozambique Channel (Manders et al., 2004), the California Bight (Lerczak et al., 2003), Portuguese Shelf (Sherwin et al., 2002), shelf off the west coast of India (Subeesh and Unnikrishnan, 2016), Virginia Slope (Nash et al., 2004), North Carolina Shelf (Savidge et al., 2007), our results also show large incoherent and unpredictable nature of internal tides on the shelf.

3.3.4 Spatial and temporal variability of semidiurnal internal tides

In this section, we describe the observed spatial and temporal variability of semidiurnal internal tides on the shelf using the computed semidiurnal internal tide variance. Time series of vertically averaged variance ($\langle u^2 \rangle + \langle v^2 \rangle$) of semidiurnal internal tides is shown in Fig. 9 and low-passed semidiurnal variance above fortnightly period is also superimposed. The semidiurnal variance averaged over 9 months on the shelf off CD, RM, KN and SG are 9.5, 3.0, 5.4 and 13.5 cm^2s^{-2} respectively. It is clear that magnitude of internal tides is large on the shelf off SG in the north,

followed by off CD in the south. Semidiurnal internal tides are relatively weak off RM and KN compared to those in other two locations. In general, the magnitudes of internal tides and their spatial and temporal variability are related to various factors such as barotropic forcing, stratification and topographic features. As mentioned earlier, barotropic tidal current gradually increases from southern to northern part of the shelf. Hence, large internal tides off SG are primarily due to the strong barotropic forcing in the north. However, even though barotropic forcing is weaker on the shelf off CD compared to those in RM and KN, internal tides are found to be strong. To explain the cause of strong internal tides off CD, location of ADCP mooring on the shelf, direction of barotropic forcing and stratification are to be considered simultaneously. Orientation of the M_2 barotropic ellipse off CD shows that barotropic forcing is in the cross-isobath direction (Fig. 3). Continental shelf on the shelf off CD is narrow (35 km) and the ADCP mooring on the shelf off CD is located close to the shelf edge. Computed criticality is close to 1, indicating that it is critical region and favourable for the generation of semidiurnal internal tides (See section 3.3.5). Relatively strong internal tides on the shelf off CD are possibly due to the proximity of generation sites of internal tides.

The internal tides are found to be strong during NE and late NE monsoon period off CD. Muller et al (2014) reported that variation of barotropic tides (M_2) about 5-10% on the continental shelf can occur due to the changes in stratification. To check the consistency of barotropic forcing in the region, monthly variance of semidiurnal barotropic currents was computed (10-14 hour bandpass) at all the locations. Results suggest that changes in the barotropic forcing are small and they are not related to semidiurnal internal tide variation (Fig. 9, right panels). Further, buoyancy frequency, computed from climatology of temperature and salinity, was used to check the stability of the water column on the shelf (Fig. 2). Computed buoyancy frequencies are large (greater than 12 cychr^{-1} at 25-100m depth) during NE monsoon and late NE monsoon period in the southern locations (off CD and RM). During SW monsoon period, northern part of the bay receives large amount of freshwater from the river run off and it enhances the near-surface stratification over there. This plume gets advected towards the south and the low salinity waters can be seen along the coast entire coast by NE monsoon period. Hence, highly stratified waters during the NE and late NE monsoon period causes strong internal tides on the shelf off CD.

Continental shelf width off RM is about 60 km and the ADCP mooring is located on the mid-shelf. Barotropic forcing on the shelf off RM is in the cross-isobath direction but semidiurnal internal tides are relatively weak. However, internal tides are found to be strong when the stratification

is high (NE monsoon). Barotropic forcing on the shelf off KN is comparable to that of off SG, however, weak cross-isobath component of barotropic tides is not favourable for the generation of strong internal tides (Fig.3). Large buoyancy frequencies (greater than 15 cyc hr^{-1} in the depth range 0-50m) in the northern location (off KN and SG) during transition months indicate highly stratified waters on the shelf during this period (Fig. 2c and d). Even though internal tides are weak on the shelf off KN, they become strong during the period of high stratification and intensify intermittently during the period of observation (Fig. 9).

On the shelf off SG, internal tides are found to be strong during the transition period when the water column is highly stratified. In an earlier study, using 2-day temperature measurements made on the shelf off Gopalpur and Visakhapatnam (17.68°N) during October 2006 and February 2007, Pradhan et al (2016) reported that strong internal tides occur during October. Interestingly, magnitude of semidiurnal internal tides off SG is substantially reduced during NE monsoon period (Fig. 9d). Similar weakening can be observed on the shelf off KN during the same period. Computed buoyancy frequencies in the subsurface (50-100 m) during NE monsoon period on the shelf off SG and KN are comparable to those in transition period. However, surface layers are weakly stratified during this period and mixed layer is found to be relatively deep (Fig. 2d). This suggests that weakly stratified waters on the shelf off KN and SG possibly reduced the magnitude of internal tides over there. Internal tides are found to be weak when stratification is low and this is particularly noticed during the beginning of SW monsoon (June) at all locations.

Monthly average of semidiurnal variance shows that variance is large at the bottom layers, indicating bottom intensification (Fig.9, right panel). For example, highest variance ($> 50 \text{ cm}^2\text{s}^{-2}$) is observed at the bottom levels off SG during the transition period (September-October). Relatively large variance at the bottom levels are also observed on the shelf off RM. In addition, large M_2 baroclinic ellipses at the bottom levels on the shelf off SG and RM (Fig. 6) further suggests the bottom intensification of internal tides in the region. A brief discussion for the bottom intensification is given in the next section.

3.3.5 Bottom Intensification of semidiurnal internal tides

Theoretical studies suggest that bottom intensification and/or generation of internal tides generally occurs at near-critical regions ($\gamma \sim c$) where the topographic slope and slope of internal wave characteristic nearly matches. This has been observed on the slope off Northwestern Spain (García-Lafuente et al., 2006), North West shelf off Australia (Holloway, 1985), Bungo Channel, Japan (Kawamura et al., 2006) and on the continental shelf off Jaigarh, west coast of India (Subeesh

and Unnikrishnan, 2016). In the present study, various analyses (Figs. 6 and 9) confirmed that semidiurnal internal tides are intensified nearly twice at the bottom levels on the shelf off SG and this feature persists during the entire period of observation. Bottom intensification is also present on the shelf off RM but with a smaller magnitude than that off SG. In the other locations (CD and KN), bottom intensification is not observed.

Based on the ratio of characteristics of internal tides (Eqs. 1 and 2), estimated from the climatology of temperature and salinity and topographic slope, we tried to infer the regions favourable for the generation of internal tides (Fig. 10). All the ADCPs are located at depths about 97-150m on the shelf and computed buoyancy frequency values from climatology in 90-150m are nearly same in all the seasons (Fig. 2). The values of buoyancy frequency at these depths (90-150 m) computed from climatology and those computed from the available temperature and salinity profiles in the region are nearly same (Fig. 10). ADCP mooring on shelf off CD is located near the shelf edge and the bathymetric slope near the mooring site is about 0.035. Results show that ADCP mooring location off CD is supercritical for semidiurnal frequencies and no bottom intensification of semidiurnal internal tides is observed (Fig. 10a). However, the internal tides off CD are found to be energetic, compared to those on the shelf off RM and off KN and they are stronger in the along-isobath direction compared to cross-isobath direction. Fig. 10a shows that near-critical regions are present offshore (depths about 400-1500 m) and north of ADCP mooring in the along isobath direction (about 4 km north). This suggests that energetic internal tides off CD could be due to the proximity of generation sites. Further, spring-neap variability and relatively large percentage of coherent internal tides (Table. 4) also indicate that internal tides are possibly generated locally near the ADCP mooring off CD. On the shelf off RM, ADCP mooring is located at about 10 km onshore from the shelf edge and the topographic slope at the mooring location is about 0.0034. Large areas near to the ADCP locations are found to be critical for semidiurnal frequencies, which possibly caused the bottom intensification of semidiurnal internal tides off RM (Fig. 10b). Continental shelf is very narrow off KN (Table 2) and the ADCP mooring is located near the shelf edge. Depth varies very rapidly across the shelf and the topographic slope is about 0.024 at the mooring location. Computed criticality shows that regions around the ADCP mooring off KN are found to be super-critical, which is not favourable for the local generation or bottom intensification of internal tides. Hence combined effect of along-isobath flow of barotropic tidal currents and super-critical regions are possibly resulting the weak internal tides off KN (Fig. 10c). The ADCP mooring location on the shelf off SG is located at about 20 km onshore of the shelf edge. The topographic slope at the ADCP mooring off SG is small (about 0.3⁰) and large areas around the ADCP location are found to

be nearly critical. The presence of near-critical regions off SG cause the bottom intensification and local generation of semidiurnal internal tides. The presence of spring-neap cycle and large percentage of coherent internal tides also indicate generation of internal tides near to the mooring location off SG (Fig. 10d). Similar characteristics of internal tides including bottom intensification is also noticed in an analysis of data from another mooring location ($85.6^{\circ}\text{E}, 19.4^{\circ}\text{N}$, the data not presented in the present study), located about 120 km northeast of SG. Further, the possibility of change in the criticality due to the seasonal variation of buoyancy frequency is examined by using monthly climatology (figure not shown), results show that there is no large shift in the critical regions because buoyancy frequency variation is small (about 1 cyc hr^{-1}) below 100 m. Based on the criticality, it appeared that weak cross-isobath component of internal tides compared to along-isobath component on the shelf off CD and off KN are possibility due to the presence of super-critical regions offshore of ADCP mooring which reflect the cross-isobath propagating internal tides to the offshore. However, more studies are required to confirm the propagation the regions in detail.

3.3.6 EOF modes and vertical shear

Complex EOF analysis was performed to obtain vertical modes of semidiurnal internal tides in cross-isobath and along-isobath directions. One of the advantage of using CEOF analysis is that it gives the spatial phase variation of EOF modes, which is useful to identify propagating features. Results of CEOF analysis carried out for the 9-month period data are presented in Fig. 11. Analysis shows that variance of the EOF first mode is found to be maximum at the bottom and near-surface level and minimum at mid-depths, which is similar to the first mode baroclinic structure. The depth of first-mode zero crossing is about 90 m on the shelf off CD. For the other locations, it lies between 50-65 m depths. The observed first-mode zero crossing depths are consistent with the mid-depth minima of M_2 baroclinic ellipses at all the locations (Fig. 6). Large contribution of the first mode to the total variance is observed on the shelf off CD (about 77%) in the south and on the shelf off SG (83%) in the north, while relatively less on the shelf off KN (46%) and RM (50%) in the central part of the coast. Compared to other locations, higher EOF modes (Mode 2, 3 and 4) are significant on the shelf off RM and KN and at least four EOF modes are required to explain about 90% of the total variance. The variance associated with higher EOF modes is large at mid depths with multiple zero crossings in the vertical. Further, EOF analysis was carried out in different seasons to check the variations of EOF modes with the seasonal change in stratification. Results show that internal tides are dominated by the first mode during all seasons at all the locations, except off KN during transition period, where the second mode is dominant. Dominant second mode structure of

M_2 internal tides can be observed on the shelf off KN from baroclinic ellipses (Fig. 6c).

The phase variation of first EOF mode on the shelf off CD in the along-isobath component shows a sudden 180° phase change between upper and lower levels, but phases for the higher modes vary gradually with depth indicating a propagating nature of higher modes. On the shelf off RM and KN, phase change is complex in different vertical levels. The phase of first EOF mode increases with depth on the shelf of SG, which indicates the downward phase propagation (upward energy propagation) of semidiurnal internal tides. The downward phase propagation of semidiurnal internal tides on the shelf off SG can also be observed from the time series (Fig. 12d). Semidiurnal internal tides on the shelf off CD do not show any phase propagation in vertical. There is no permanent pattern in the vertical phase propagation observed at other ADCP locations (Fig. 11b and c) and inconsistency in the phase propagation over time indicates the complex nature of semidiurnal internal tide propagation.

Internal tides cause vertical mixing due to small-scale shear. Cross-isobath and along-isobath internal tidal currents show complicated vertical structure due to the presence of multi-modes of internal tides on the shelf (Fig. 12). The computed total vertical shear ($(\partial u/\partial z)^2 + (\partial v/\partial z)^2$) for semidiurnal internal tides for a 20-day period is presented in Fig. 12. Vertical shear by semidiurnal internal tides is high at mid depths at different stations and this is typical for first mode internal tides. Large shear can be observed at the depth of first mode zero crossing on the shelf off CD. However, in the northern locations, large vertical shear ($>10^{-2} \text{ s}^{-1}$) is observed close to the bottom and surface. Enhanced vertical shear is found in the regions of bottom intensification. Vertically-averaged shear becomes strong when the semidiurnal internal tides are intense (figure not shown). Presence of multimode internal tides causes large shear at various vertical levels. For example, time series of semidiurnal internal tides on the shelf off CD and KN during 5-11 November 2010 show multimodal vertical structure (Fig. 12a and c). The semidiurnal shear during the same period is found to be enhanced due to higher mode internal tides. To confirm the presence of the vertical shear at various depths caused by higher modes, vertical shear associated with different EOF modes was computed (mode-1, 2, 3 and 4) and found large shear in the depths of zero-crossings of different modes. Similar events of enhancement of semidiurnal shear caused by higher-mode internal tides is observed at all the ADCP locations during the period of observation.

4. Discussion and conclusion

In this paper, current measurements for a 9-month period (June to February), carried out during 2009-2013 using ADCPs deployed at four locations on the continental shelf off the east coast

of India were used to study the barotropic and internal tides in the region. The major results and conclusions of the present study are summarised below.

4.1 Barotropic tidal currents

Observed tidal currents along the shelf off the east coast of India are predominantly semidiurnal in nature and magnitude of barotropic M_2 tidal currents gradually increases from the southern to northern parts of the shelf. Continental shelf along the east coast is narrow and the shelf width varies intermittently (Table 2). Co-range charts of M_2 and S_2 in the BoB show that their amplitudes gradually increase from southern to northern parts of the bay and in the head of the bay, they get amplified nearly twice on a very wide continental shelf (Sindhu and Unnikrishnan, 2013), according to the theory of Clarke and Battisti(1981) on the amplification of semidiurnal tides over wide continental shelves in non-polar latitudes. Tidal ellipses are oriented nearly in a cross-isobath direction on the shelf off CD, RM and SG. In the central part of the east coast of India, between RM and SG, the coastline is oriented in a north-east direction and the tidal currents (off KN, for instance) tend to flow parallel to the coast in an along-isobath direction with anticlockwise rotation. Based on the studies of Battisti and Clarke (1982), tidal currents get oriented in an along-isobath direction on the narrow continental shelves and tidal currents rotate in an anticlockwise direction if the frictional influence is small. It is possible that narrow continental shelf (about 30 km) and orientation of the coastline caused the along-isobath flow of tidal currents off KN. A comparison of observed tidal currents with those from TPXO7.2 tidal model shows a good consistency in phase, but the latter underestimates the magnitudes.

4.2 Semidiurnal internal tides on the shelf

Analyses of ADCP data reveal that internal tides on the shelf off east coast of India are dominated by semidiurnal internal tides with magnitudes of about $8-15 \text{ cms}^{-1}$. Diurnal internal tides are relatively weak ($2-4 \text{ cms}^{-1}$) on the shelf. Predominance of spectral energy at tidal frequencies, particularly in the semidiurnal band show that energetic internal wave motions in the region are mostly confined to semidiurnal internal tides. Semidiurnal internal tides are found to be strong on the shelf off SG, the northernmost location, where it contributes to about 20% of the total baroclinic current followed by off CD (the southernmost location), where it is about 17%. On the shelf off KN and RM, internal tides are weak and the contribution of semidiurnal internal tides to total baroclinic current is about 10%. Maximum magnitude of semidiurnal internal tides are observed in the northern most location (off SG) with a cross-isobath velocity of about $10-15 \text{ cms}^{-1}$ which is primarily due to large barotropic forcing in the north compared to southern part of the shelf. The semidiurnal internal

tides are found to be nearly twice intensified at bottom levels compared to surface in this location. Similar intensification is also observed on the shelf off RM but with a small magnitudes. The computed ratio of topographic slope and slope of internal wave characteristics show the presence of large area surrounding the ADCP moorings off SG and RM, critical for the generation of semidiurnal internal tides. These conditions also favour for the bottom intensification of semidiurnal internal tides. Even though the barotropic forcing is weak in the southern part, energetic internal tides are observed on the shelf off CD. Computed criticality shows that the near-critical regions are present near to the mooring location off CD and energetic internal tides results in the presence of proximity of generation sites. Further, based on the criticality, it appeared that weak cross-isobath component of internal tides compared to along-isobath component on the shelf off CD and off KN are possibly due to the presence of super-critical regions offshore of ADCP mooring which reflect the cross-isobath propagating internal tides to the offshore. However, more studies are required to confirm the propagation of internal tides in the region in detail.

EOF analysis show that observed semidiurnal internal tides are dominated by the first mode on the shelf. The first EOF mode accounts for about 70-80 % of semidiurnal internal tide variability on the shelf off SG and CD, whereas it is relatively small (43-50%) on the shelf off KN and RM. Higher modes are significant on the shelf off RM and KN. Large small-scale vertical shear ($> 10^{-2} \text{ s}^{-1}$) is observed at various vertical levels associated with different modes of semidiurnal internal in all locations (Fig. 12). In addition, vertical shear is found to be enhanced due to the presence of higher mode semidiurnal internal tides on the shelf.

Semidiurnal internal tides show a spring-neap variability on the shelf off SG and CD, but they are highly incoherent and intermittent the shelf off RM and KN. Previous studies point out that varying background stratification, low-frequency currents, mesoscale eddies and remotely generated shoaling internal tides could alter the local internal wave field and eventually cause incoherent and intermittent internal tides (Rainville and Pinkel, 2006; Kelly and Nash, 2010; Ponte and Klein, 2015). Numerical modelling studies carried out by Pradhan et al. (2016) reported that the seasonal changes in stratification off the east coast of India cause the shift in the location of peak spectral energy of internal tides across the shelf. In the present study, we tried to explain the temporal variability of internal tides on the shelf based on the changes in stratification using monthly climatology. Semidiurnal internal tides are found to be small in the beginning of SW monsoon period (June) due to weakly stratified waters on the shelf. In the southern part of the shelf (off CD and RM), internal tides are found to be intensified during NE and late NE monsoon due to the strong vertical

stratification. Maximum magnitudes of semidiurnal internal tides in the northern part of the shelf (off SG and KN) are observed during the transition period (Sep-Oct) due to the high stratification. During SW monsoon, mixed layer is shallow off the north east coast of India and the mixed layer deepens during NE monsoon (Shetye et al., 1996; Thadathil et al., 2002). Deepening of the mixed layer during NE monsoon causes well mixed water on the shelf off SG which possibly reduced the internal tide activity in the region. There are few instances of the presence of energetic internal tides for instance, off SG during late NE monsoon, which cannot be explained in terms of the seasonal evolution of stratification from climatological field of temperature and salinity. However, the internal tides off SG during this period (Jan-Feb) are not as energetic as those found during the SW monsoon and transition periods (Fig.9). Studies in the other regions indicate that internal tide variability can result from various factors such as, changes in the sub-tidal circulation (Kerry et al., 2013), variations in the depth of pycnocline (Mitchum and Chiswell, 2000), the presence of density fronts (Chaung and Wang, 1981) and meso-scale eddies (Park and Watts, 2006). These factors can also be true in the case of internal tide variability on the shelf off the east coast of India. The region off the east coast of India is very dynamic with the presence of a strong western boundary current (EICC) which shows large seasonal and intra seasonal variability (Mukherjee et al., 2013). The region is also characterised by low surface salinity due to the large fresh water discharge from the rivers which enhances the near-surface stratification. Earlier studies reported the presence of coastal thermohaline fronts with strong vertical and lateral density gradients between the shelf and slope (Kumar et al., 2013). Temperature inversions and barrier layer formations are prominent in this region (Thadathil et al., 2002, 2007), which can also lead to the changes in stratification. In addition, western BoB is also well known for the presence of mesoscale eddies and they can alter the vertical structure of temperature/salinity and eventually modify the stratification (Patnaik et al., 2016; Rayaroth et al., 2016). In short, varying background conditions in the region might alter the vertical structure of temperature and salinity in different time scales and results temporal variations in the internal tide field. Detailed studies are required to understand the effect of various processes on the internal tide variability on the shelf and we plan to address some of these questions using a numerical model in an ongoing study.

Acknowledgements

The funding for the ADCP moorings was provided by CSIR-National Institute of Oceanography (NIO), Goa and the Indian National Centre for Ocean Information Services (INCOIS), Hyderabad, Ministry of Earth Sciences. The present work is the part of the project 'Tidal currents off the Indian

coasts' funded by INCOIS. We acknowledge the officers and crew members of the research vessels for their support during the deployment and retrieval of ADCP. We are grateful to USGS for providing their ADCP tool box (<http://woodshole.er.usgs.gov/operations/stg/pubs/ADCPtools/adcpindex.htm>). The USGS MATLAB code was converted to Octave and C by A. Krishnakiran, R. Fernandes, S.P. Vernekar and N. Nasnodkar. The first author thanks to Arnab Mukherjee for discussions. The Authors thank Michael G S and NIO data centre for providing temperature and salinity data. Bathymetry data (SRTM30_PLUS) were downloaded from ftp://topex.ucsd.edu/pub/srtm30_plus and TPXO7.2 model is downloaded from <http://volkov.oce.orst.edu/tides/>. All figures were made using Generic Mapping tool (GMT) and analysis was carried out by using FORTRAN, MATLAB and FERRET. This is NIO contribution No:XXXX.

References

- Baines, P.G., 1982. On internal tide generation models. *Deep Sea Research. Part A* 29 (3), 307–338. doi:10.1016/0198-0149(82)90098-X.
- Battisti, D.D., Clarke, A.J., 1982. A simple method for estimating barotropic tidal currents on the continental margins with specific application to the M2 tide off the Atlantic and Pacific coast of the United States. *Journal of Physical Oceanography*. 12, 8-16. doi: 10.1175/1520-0485(1982)012<0008;ASMFEB>2.0.CO;2.
- Bravo, L., Ramos, M., Sobarzo, M., Pizarro, O., Valle Levinson, A., 2013. Barotropic and baroclinic semidiurnal tidal currents in two contrasting coastal upwelling zones of Chile. *Journal of Geophysical Research-Oceans*. 118(3), pp.1226-1238. doi:10.1002/jgrc.20128.
- Chaitanya, A.V.S., Lengaigne, M., Vialard, J., Gopalakrishna, V.V., Durand, F., Kranthikumar, C., Amritash, S., Suneel, V., Papa, F., Ravichandran, M., 2014. Salinity Measurements Collected by Fishermen Reveal a “River in the Sea” Flowing Along the Eastern Coast of India. *Bulletin of the American meteorological Society*. 95(12), pp.1897-1908. doi:10.1175/BAMS-D-12-00243.1.
- Chatterjee, A., Shankar, D., Shenoi, S.S.C., Reddy, G.V., Michael, G.S., Ravichandran, M., Gopalakrishna, V.V., Rao, E.P.R., Bhaskar, T.V.S.U., Sanjeevan, V.N., 2012. New atlas of temperature and salinity for North Indian Ocean. *Journal of Earth System Science*, 121 (3) (2012), pp. 559–593. doi:10.1016/j.csr.2013.09.008.
- Chuang, W.S., Wang, D.P., 1981. Effects of density front on the generation and propagation of internal tides. *Journal of Physical Oceanography*. 11(10), pp.1357-1374.
- Clarke, A.J., Battisti, D.S., 1981. The effect of continental shelves on tides. *Deep Sea Research. Part A* 28(7), pp.665-682. doi: 10.1016/0198-0149(81)90128-X.
- Egbert, G.D., Ray, R.D., 2000. Significant dissipation of tidal energy in the deep ocean inferred from satellite altimeter data. *Nature*. 405(6788), pp.775-778. doi:10.1038/35015531.

- García-Lafuente, J., delRío, G.D., Berrocal, C.S., 2006. Vertical structure and bottom-intensification of tidal currents off Northwestern Spain. *Journal of Marine Systems*. 62(1), pp.55-70. doi:10.1016/j.jmarsys.2006.04.006.
- Gill, A., 1982. *Atmosphere–Ocean Dynamics*. Academic Press, New York.
- Guo, P., Fang, W., Liu, C., Qiu, F., 2012. Seasonal characteristics of internal tides on the continental shelf in the northern South China Sea. *Journal of Geophysical Research- Oceans*, 117, C04023, doi:10.1029/2011JC007215.
- Holloway, P.E., 1985. A comparison of semidiurnal internal tides from different bathymetric locations on the Australian North West Shelf. *Journal of Physical Oceanography*. 15, 240–251. doi:10.1175/1520-0485(1985)015<0240:ACOSIT>2.0.CO;2.
- Kawamura, Y., Hayami, Y., Kohama, T., Kaneda, A., Takeoka, H., 2006. Occasional intensification of semidiurnal internal tide in Bungo Channel, Japan. *Geophysical Research Letters*, 33(14).doi:10.1029/2006GL025866.
- Kelly, S.M., Nash, J.D., 2010. Internal-tide generation and destruction by shoaling internal tides. *Geophysical Research Letters*. 37, L23611. doi:10.1029/2010GL045598.
- Kerry, C.G., Powell, B.S., Carter, G.S., 2013. Effects of remote generation sites on model estimates of M_2 internal tides in the Philippine Sea. *Journal of Physical Oceanography*. 43, 187–204. doi:10.1175/JPO-D-12-081.1.
- Kumar, P.V.H., Mathew, B., Kumar, M.R.R., Rao, A.R., Jagadeesh, P.S.V., Radhakrishnan, K.G., Shyni, T.N., 2013. ‘Thermohaline front’ off the east coast of India and its generating mechanism. *Ocean Dynamics*. 63(11-12),pp.1175-1180. doi:10.1007/s10236-013 -0652-y.
- Kumar, P.V.H., Rao, C.V.K.P., Swain, J., Madhusoodanan, P., 2001. Intra-seasonal oscillations in the central Bay of Bengal during summer monsoon 1999. *Current Science-Bangalore*. 80(6), pp.786-790.
- LaFond, K.G., Rao, C.P., 1954. Vertical Oscillations of Tidal Periods in the Temperature Structure of the Sea. In *Andhra University Memoirs* 1, pp.109-116.
- Lerczak, J.A., Winant, C.D., Hendershott, M.C., 2003. Observations of the semidiurnal internal tide on the southern California slope and shelf. *Journal of Geophysical Research-Ocean*. 108, 3068. doi:10.1029/2001JC001128.
- Manders, A.M.M., Maas, L.R.M., Gerkema, T., 2004. Observations of internal tides in the Mozambique Channel. *Journal of Geophysical Research-Oceans*. 109, C12034. doi:10.1029/2003JC002187.
- Misra S.K., Chandramohan, P., SatyanarayanaMurty, A., Panigrahi, J.K., Mahadevan, R., 2013. Nature of the tide induced flow field along the East Coast of India. *International Journal of Oceans and Oceanography*. ISSN 0973-2667 Vol.7, No.1, pp. 57-71.
- Misra, S.K., Chandramohan, P., SatyanarayanaMurty, A., 2011. Numerical simulation of tide, wind and storm induced current off Chennai Coast. *An international Quarterly Journal of Environmental Sciences*. pp.119-123.

- Mitchum, G.T., Chiswell, S.M., 2000. Coherence of internal tide modulations along the Hawaiian Ridge. *Journal of Geophysical Research-Oceans*. 105(C12), pp.28653- 28661.
- Mukherjee, A., Shankar, D., Aparna, S.G., Amol, P., Fernando, V., Fernandes, R., Khalap, S., Narayan, S., Agarvadekar, Y., Gaonkar, M., Tari, P., Kankonkar, A., Vernekar, S., 2013. Near-inertial currents off the east coast of India. *Continental Shelf Research*. 55, 29–39. doi:10.1016/j.csr.2013.01.007.
- Mukherjee, A., Shankar, D., Fernando, V., Amol, P., Aparna, S.G., Fernandes, R., Michael, G.S., Khalap, S.T., Satelkar, N.P., Agarvadekar, Y., Gaonkar, M.G., 2014. Observed seasonal and intraseasonal variability of the East India Coastal Current on the continental slope. *Journal of Earth System Science*. 123(6), pp.1197- 1232. doi:10.1007/s12040-014-0471-7.
- Murty, T.S., Henry, R.F., 1983. Tides in the Bay of Bengal. *Journal of Geophysical Research*. Vol. 88, July 20, No. C10, 6069-6076. doi:10.1029/JC088iC10p06069.
- Nash, J. D., Kunze, E., Toole, J.M., Schmitt, R.W., 2004. Internal tide reflection and turbulent mixing on the continental slope. *Journal of Physical Oceanography*. 34, 1117–1134.
- Nash, J.D., Shroyer, E.L., Kelly, S.M., Inall, M.E., Duda, E.T.F., Levine, M.D., Jones, N.L and Musgrave, R.C., 2012. Are any coastal internal tides predictable? *Oceanography*. 25(2):80–95, <http://dx.doi.org/10.5670/oceanog.2012.44>.
- Papa, F., Bala, S.K., Pandey, R.K., Durand, F., Gopalakrishna, V.V., Rahman, A., Rossow, W.B., 2012. Ganga-Brahmaputra river discharge from Jason-2 radar altimetry: An update to the long-term satellite-derived estimates of continental freshwater forcing flux into the Bay of Bengal. *Journal of Geophysical Research-Oceans*. 117(C11). doi:10.1029/2012JC008158.
- Park, J.H., Watts, D.R., 2006. Internal tides in the southwestern Japan/East Sea. *Journal of Physical Oceanography*, 36(1), pp.22-34.
- Patnaik, K.V.K.R.K., Maneesha, K., Sadhuram, Y., Prasad, K.V.S.R., RamanaMurty, T.V., Brahmananda Rao, V., 2014. East India Coastal Current induced eddies and their interaction with tropical storms over Bay of Bengal. *Journal of Operational Oceanography*. 7(1), pp.58-68. doi: 10.1080/1755876X.2014.11020153.
- Pawlowicz, R., Beardsley, B., Lentz, S., 2002. Classical tidal harmonic analysis including error estimates in MATLAB using T_TIDE. *Computers & Geosciences*, 28(8), pp.929-937. doi:10.1016/S0098-3004(02)00013-4.
- Pingree, R.D., Mardell, G.T., New, A.L., 1986. Propagation of internal tides from the upper slopes of the Bay of Biscay. *Nature*. 321, 8 May, 154-158. doi:10.1038/321154a0.
- Ponte, A. L., Klein, P., 2015. Incoherent signature of internal tides on sea level in idealized numerical simulations. *Geophysical Research Letters*. 42, 1520–1526, doi:10.1002/2014GL062583.
- Pradhan, H.K., Joshi, M., Rao, A.D., 2013. Simulation of internal waves in the western Bay of Bengal using MITGCM: A case study. In *OCEANS-Bergen, MTS/IEEE* (pp. 15).IEEE. doi:10.1109/OCEANS-Bergen.2013.6607966.

- Pradhan, H.K., Rao, A.D., Joshi, M., 2016. Neap—spring variability of internal waves over the shelf-slope along western Bay of Bengal associated with local stratification. *Natural Hazards*. 80(2), pp.1369-1380. doi:10.1007/s11069-015-2027-9.
- Prasad, K.V.S.R., Rajasekhar, M., 2010. Space borne SAR observations of oceanic internal waves in North Bay of Bengal. *Natural hazards*. 57(3), pp.657-667. doi:10.1007/s11069-010-9630-6.
- Rainville, L., Robert Pinkel., 2006. Propagation of Low-Mode Internal Waves through the Ocean. *Journal of Physical Oceanography*. Vol.36, pages-1220-1236. doi:10.1175/JPO2889.1.
- Rao, A.D., Babu, S.V., Murty, P.L.N., Pandey, S., 2011. Impact of stratification on internal waves and differential wearing of thermal inversions on the east coast of India. *Natural hazards*. 57(3), pp.577-595. doi:10.1007/s11069-010-9616-4
- Rao, A.D., Babu, S.V., Prasad, K.V.S.R., Murty, T.R., Sadharam, Y., Mahapatra, D.K., 2010. Investigation of the generation and propagation of low frequency internal waves: a case study for the east coast of India. *Estuarine, Coastal and Shelf Science*. 88(1), pp.143-152. doi:10.1007/s11069-010-9616-4.
- Rayaroth, M.K., Peter, B.N., Mahmud, M.R., 2016. High resolution surface circulation of the Bay of Bengal derived from satellite observation data. *Journal of Marine Science and Technology*. Vol. 24, No. 3, pp. 656-668 (2016). doi 10.6119/JMST-015-1215-2.
- Sarma, Y.V.B., Sarma, M.S.S., Charyulu, R.J.K., Rao, D.P., 1991. Subsurface oscillations at an oceanic station in the Bay of Bengal. *Indian Journal of Marine Science*. September, vol. 20, 204-207.
- Sarma, M.S.S., Rao, L.G., 1989. Spectra of currents and temperature off Godavari (east coast of India). *Mahasagar*. 22(1), pp.29-36.
- Savidge, D., Edwards, C., Santana, M., 2007. Baroclinic effects and tides on the Cape Hatteras continental shelf. *Journal of Geophysical Research-Oceans*. 112, C09016. doi:10.1029/2006JC003832.
- Sherwin, T.J., Vlasenko, V.I., Stashchuk, N., Jeans, D.R., Jones, B., 2002. Along-slope generation as an explanation for some unusually large internal tides. *Deep Sea Research Part I* 49:1,787–1,799. [http://dx.doi.org/10.1016/S0967-0637\(02\)00096-1](http://dx.doi.org/10.1016/S0967-0637(02)00096-1).
- Shetye, S.R., Gouveia, A.D., Shankar, D., Shenoi, S.S.C., Vinayachandran, P.N., Sundar, D., Michael, G.S., Nampoothiri, G., 1996. Hydrography and circulation in the western Bay of Bengal during the northeast monsoon. *Journal of Geophysical Research- Oceans*. 101(C6), pp.14011-14025. doi:10.1029/95JC03307.
- Shetye, S.R., Shenoi, S.S.C., Gouveia, A.D., Michael, G.S., Sundar, D., Nampoothiri, G., 1991. Wind-driven coastal upwelling along the western boundary of the Bay of Bengal during the southwest monsoon. *Continental Shelf Research*. 11(11), pp.1397-1408. doi:10.1016/0278-4343(91)90042-5.
- Sindhu, B., A. S. Unnikrishnan., 2013. Characteristics of Tides in the Bay of Bengal. *Marine*

Geodesy. 36:4, 377-407. doi: 10.1080/01490419.2013.781088.

Sridevi, B., Murty, T.R., Sadhuram, Y., Rao, M.M.M., Maneesha, K., Kumar, S.S., Prasanna, P.L., 2010. Impact of internal waves on sound propagation off Bhimilipatnam, east coast of India. *Estuarine, Coastal and Shelf Science*. 88(2), pp.249-259. doi:10.1016/j.ecss.2010.03.020.

Subeesh, M.P., Unnikrishnan, A.S., 2016. Observed internal tides and near-inertial waves on the continental shelf and slope off Jaigarh, central west coast of India. *Journal of Marine Systems*. 157, pp.1-19. doi:10.1016/j.jmarsys.2015.12.005.

Subeesh, M.P., Unnikrishnan, A.S., Fernando, V., Agarwadekar, Y., Khalap, S.T., Satelkar, N.P., Shenoi, S.S.C., 2013. Observed tidal currents on the continental shelf off the west coast of India. *Continental Shelf Research*. 69, 123-140. doi:10.1016/j.csr.2013.09.008.

Thadathil, P., Muraleedharan, P. M., Rao, R. R., Somayajulu, Y. K., Reddy, G. V., Revichandran, C., 2007. Observed seasonal variability of barrier layer in the Bay of Bengal. *Journal of Geophysical Research-Oceans*. 112, C02009, doi:10.1029/2006JC003651.

Thadathil, P., Gopalakrishna, V., Muraleedharan P.M., Reddy, G.V., Araligidat, N., Shenoy, S., 2002. Surface layer temperature inversion in the Bay of Bengal. *Deep Sea Research Part I*. 49:1801-1818.

Wunsch, C., 1975. Internal tides in the ocean. *Reviews of Geophysics*. Feb 1;13(1):167-82. doi:10.1029/RG013i001p00167.

Figures

Fig. 1: Map showing the locations of four ADCP moorings on the shelf in the Bay of Bengal used in the present study. Red circles show the location of ADCP mooring on shelf. Depth contours of 100 m, 1000 m and 2000 m are also shown. The short forms of ADCP stations off Cuddalore, Ramayapatnam, Kakinada and South of Gopalpur are CD, RM, KN and SG respectively.

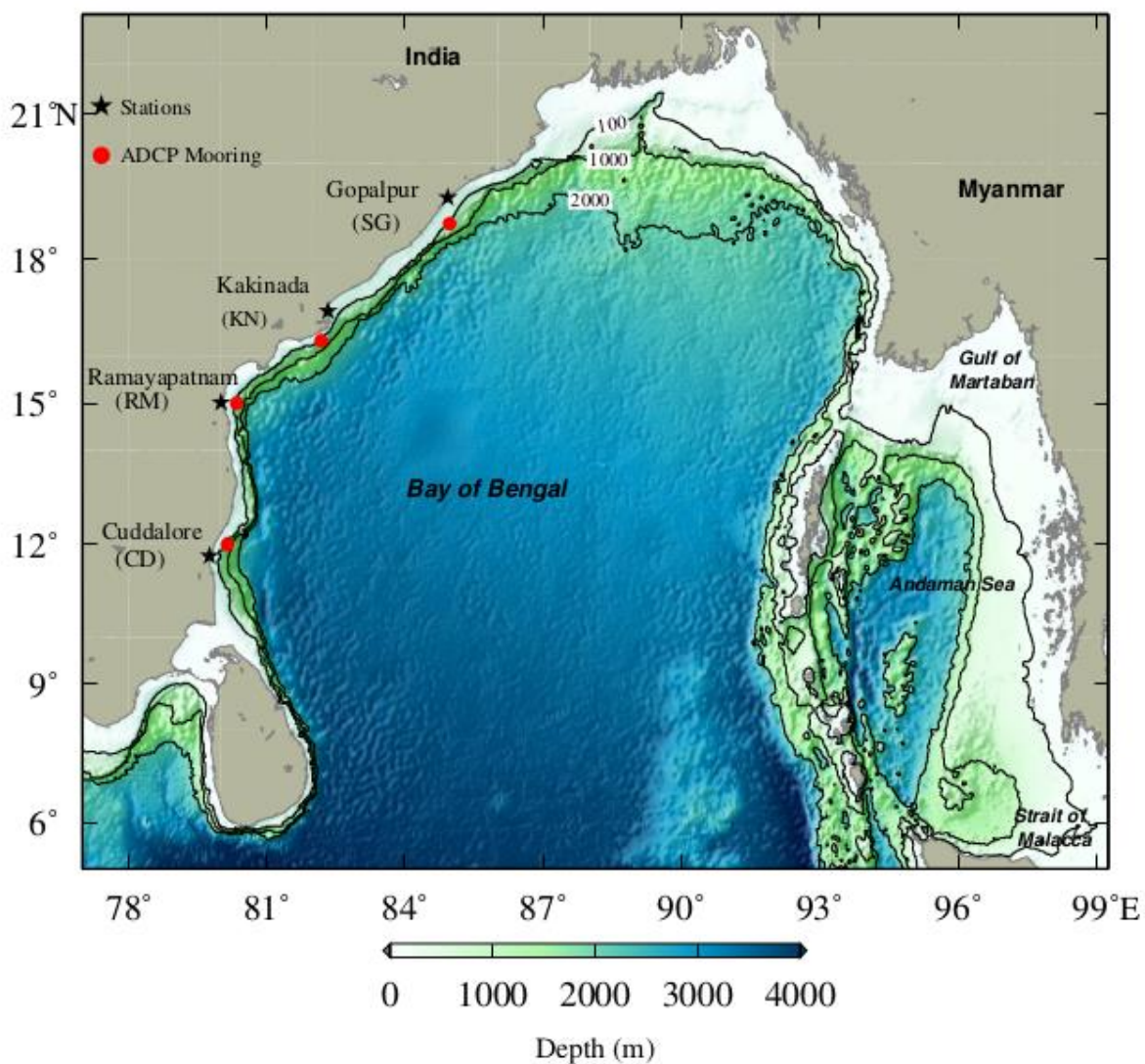


Fig. 2: Variation of buoyancy frequency (N) at depths of 0-150 m from June to February calculated using Eq. 2 from the revised climatology for North Indian Ocean (Chatterjee et al., 2012) off (a) CD, (b) RM, (c) KN and (d) SG. The contours show the potential density (σ_θ) in the vertical levels computed from the climatology.

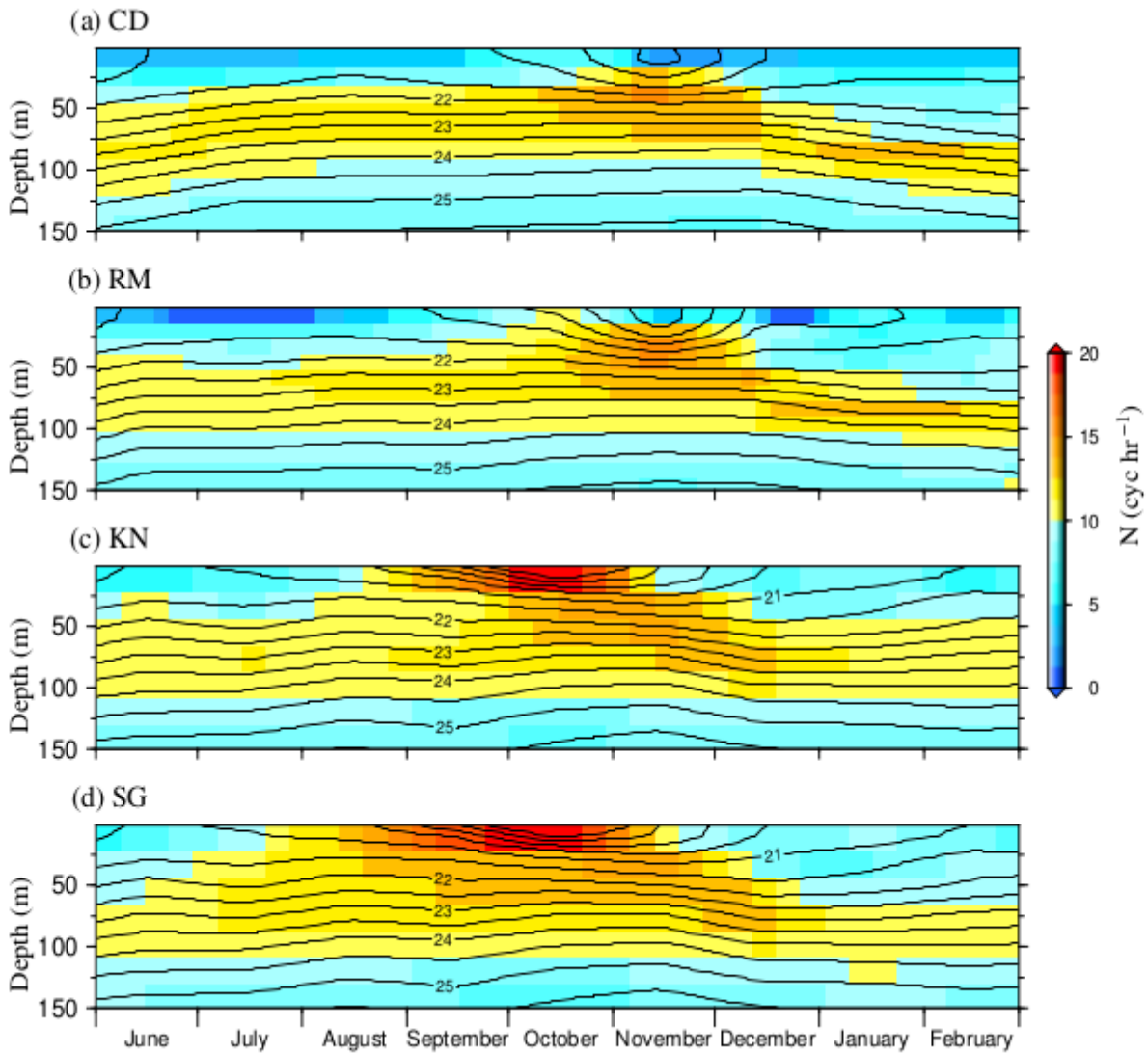


Fig. 3: Barotropic tidal ellipses for (a) M_2 and (b) S_2 obtained from harmonic analysis of 9-month period. Solid line from the centre of ellipse represent the phase (g) and black arrow on the ellipse indicate the sense of rotation of the ellipse. Depth contours of 100 m, 1000 m and 3000 m are also shown.

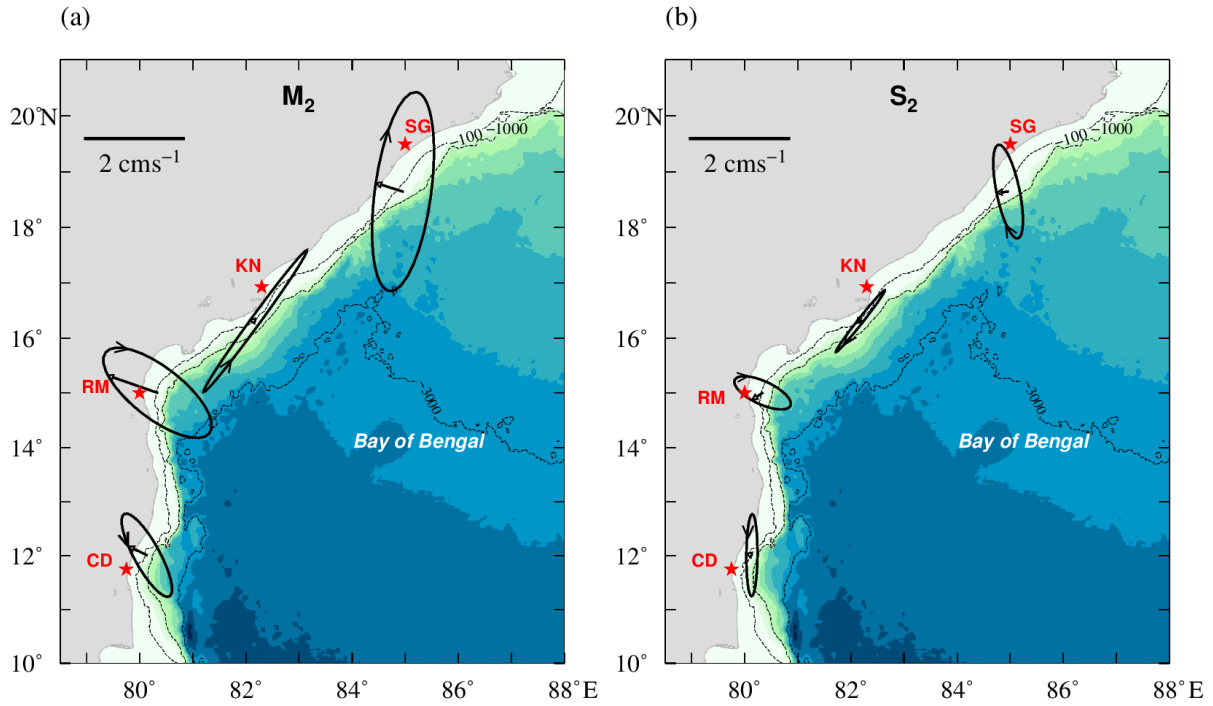


Fig. 4: Time series of northward and eastward component of observed (red) barotropic tidal current obtained from harmonic analysis and tidal currents extracted from TPXO7.2 model (blue) at four ADCP locations on the shelf.

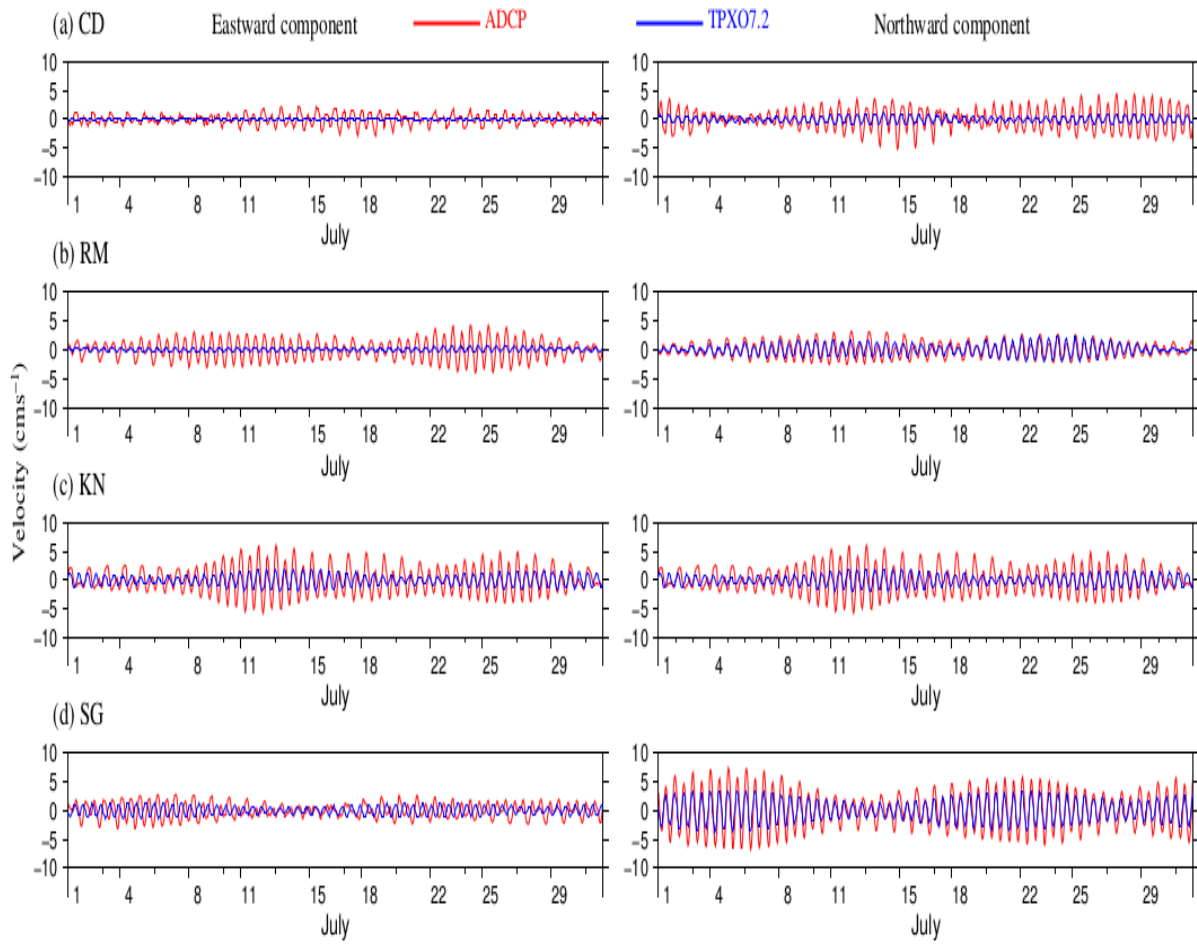


Fig. 5: Clockwise (red) and anticlockwise (blue) components of rotary spectra of the baroclinic horizontal currents on the shelf off (a) CD, (b) RM, (c) KN and (d) SG. Spectra were determined using the entire period of observations (June-February) and vertically averaged. Vertical black dotted line represents the tidal frequencies and inertial frequency (f). Grey shaded region in the spectra represents the semidiurnal band (10-14 hour) and confidence interval of 95% of the spectra are also shown.

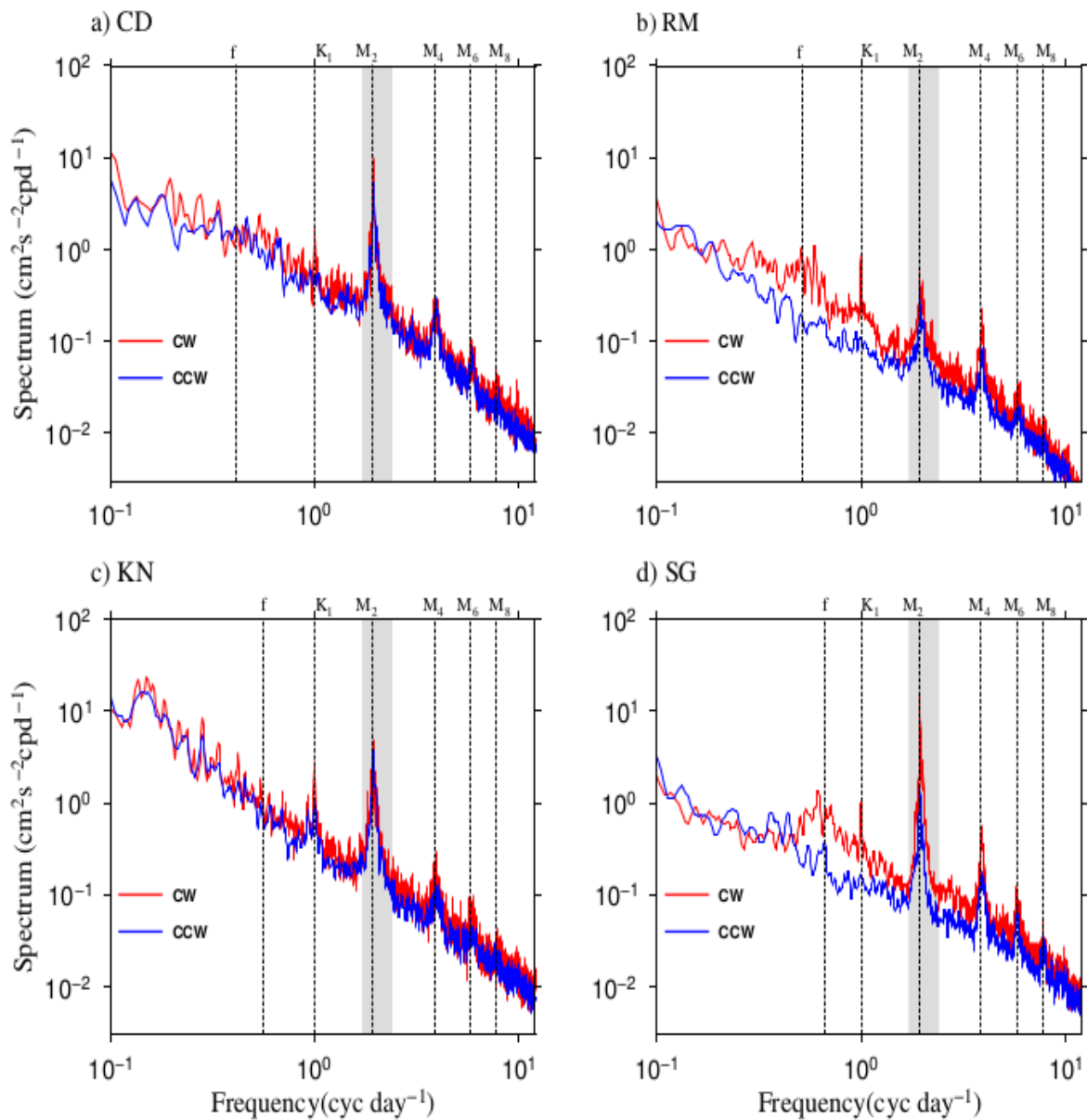


Fig. 6: Baroclinic M_2 tidal ellipses on the shelf off (a) CD, (b) RM, (c) KN and (d) SG obtained from the harmonic analysis of two-month data during July-August, September-October, November-December and January-February. Solid line from the centre of ellipse represents the local phase (ϕ). Sense of rotation of ellipses are shown in black and grey for clockwise and anticlockwise rotation respectively. M_2 ellipse parameters obtained from t_{tide} with signal-noise ratio less than 1 are considered as statistically insignificant and those ellipses are shown in dotted lines. Depth at the mooring location is indicated by an arrow pointing to the Y-axis.

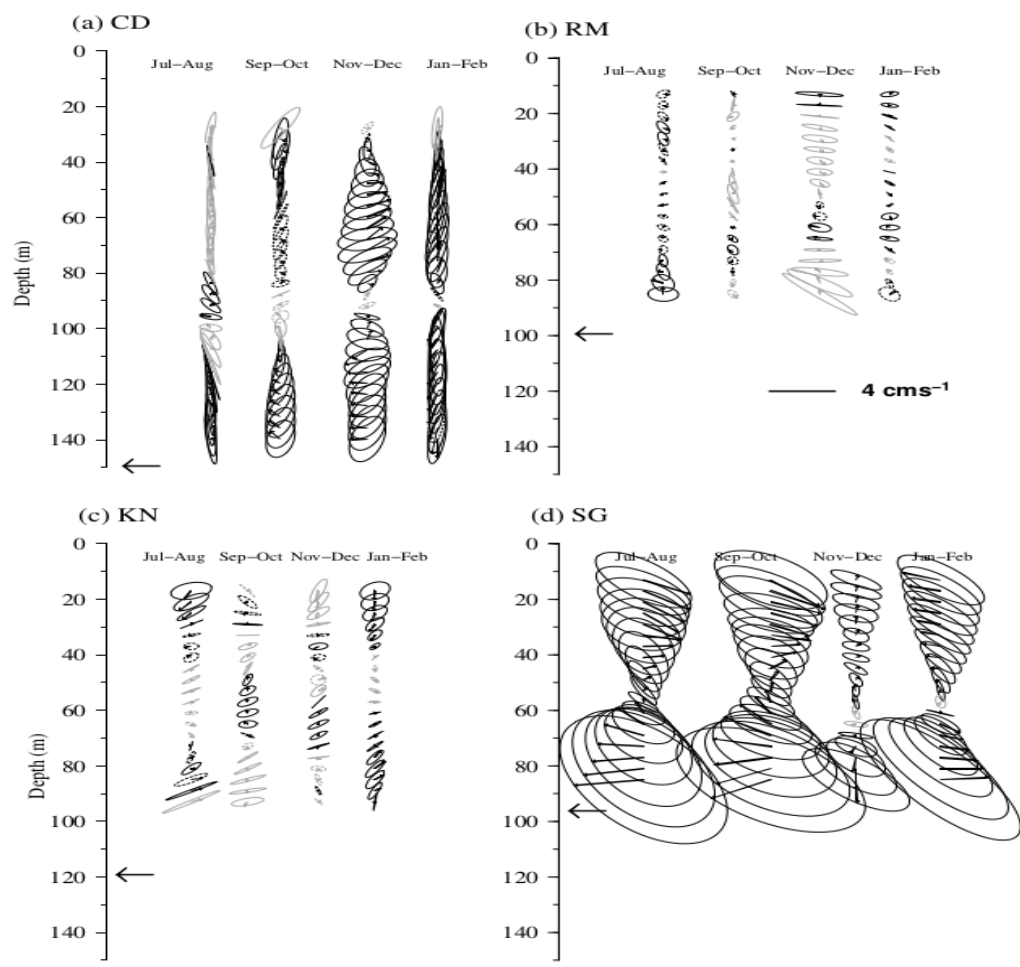


Fig. 7: Time series of band-passed (10-14 hour) cross-isobath (red) and along-isobath (blue) semidiurnal internal tides on the shelf off (a) CD, (b) RM, (c) KN and (d) SG. Depths of given time series are also indicated in the figure. Band-passed barotropic semidiurnal tidal currents from ADCP observations and tidal elevations obtained from TPXO7.2 model in the same period at all the ADCP locations are also presented.

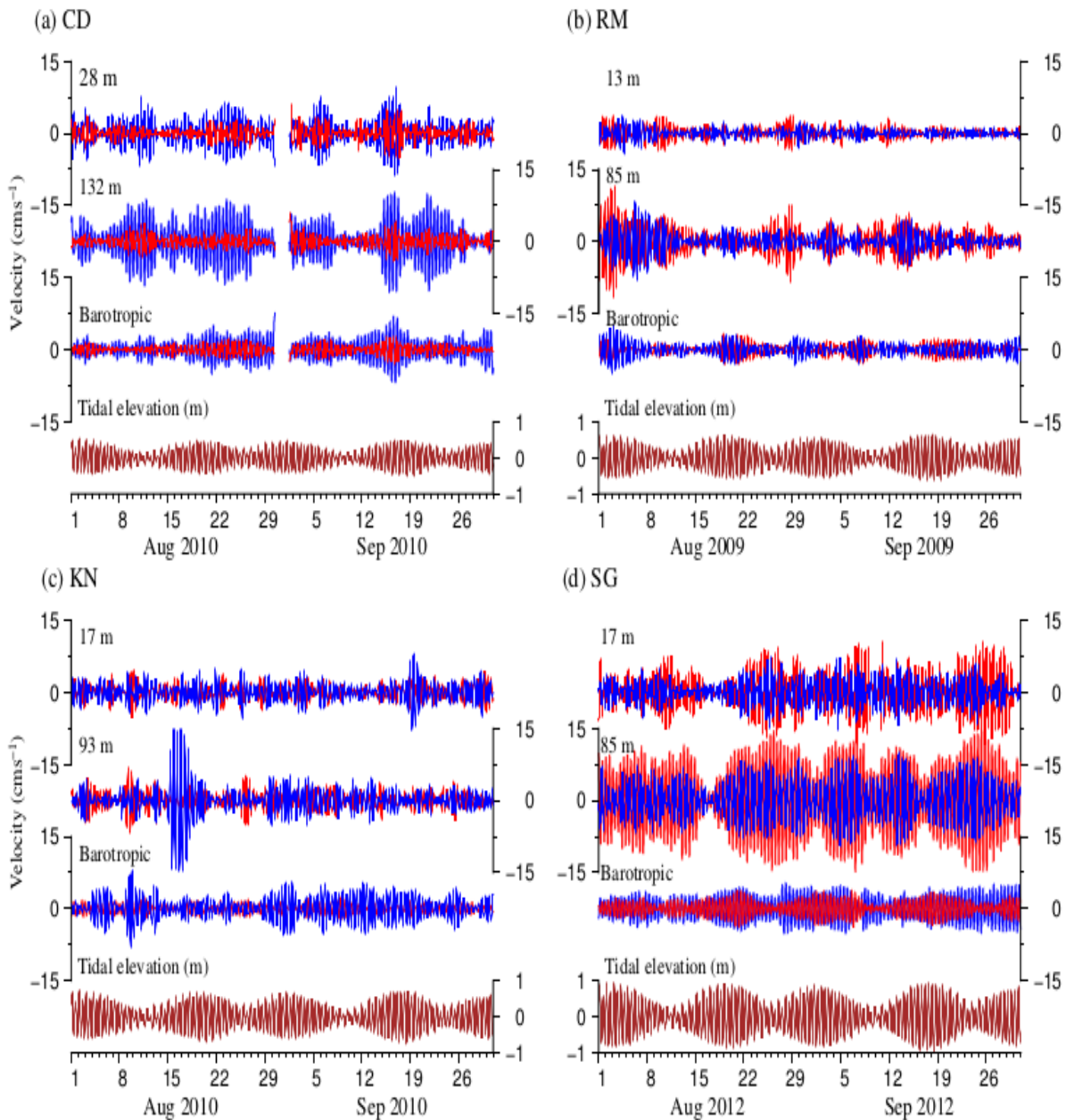


Fig. 8: Variance ($\langle u^2 \rangle + \langle v^2 \rangle$) of semidiurnal internal tide (blue, given as coherent) obtained from the one month harmonic analysis of the semidiurnal band-passed (10-14 hour) current and incoherent semidiurnal internal tide variance (red) on the shelf off (a) CD, (b) RM, (c) KN and (d) SG.

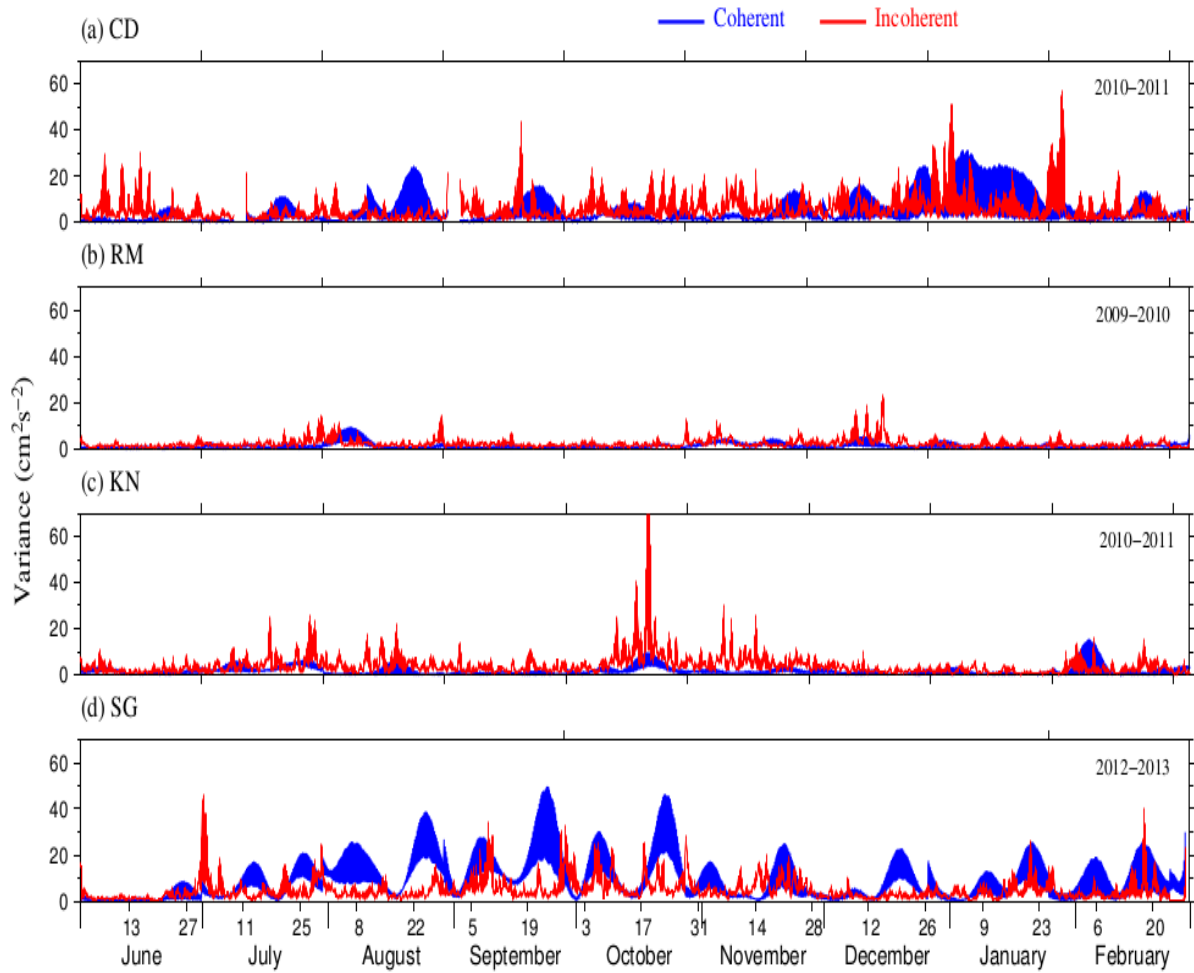


Fig. 9: Vertically averaged variance ($\langle u^2 \rangle + \langle v^2 \rangle$) of semidiurnal internal tides at different locations on the shelf. Red line shows the low frequency variability of semidiurnal variance obtained by low-pass filtering with a 15-day period cut-off. The right panels represent the monthly average of semidiurnal internal tide variance (continuous lines) and semidiurnal barotropic current variance (dashed vertical lines) during August (blue), October (black), December (green) and February (red). Note that X-axis scaling in the right panel is not uniform.

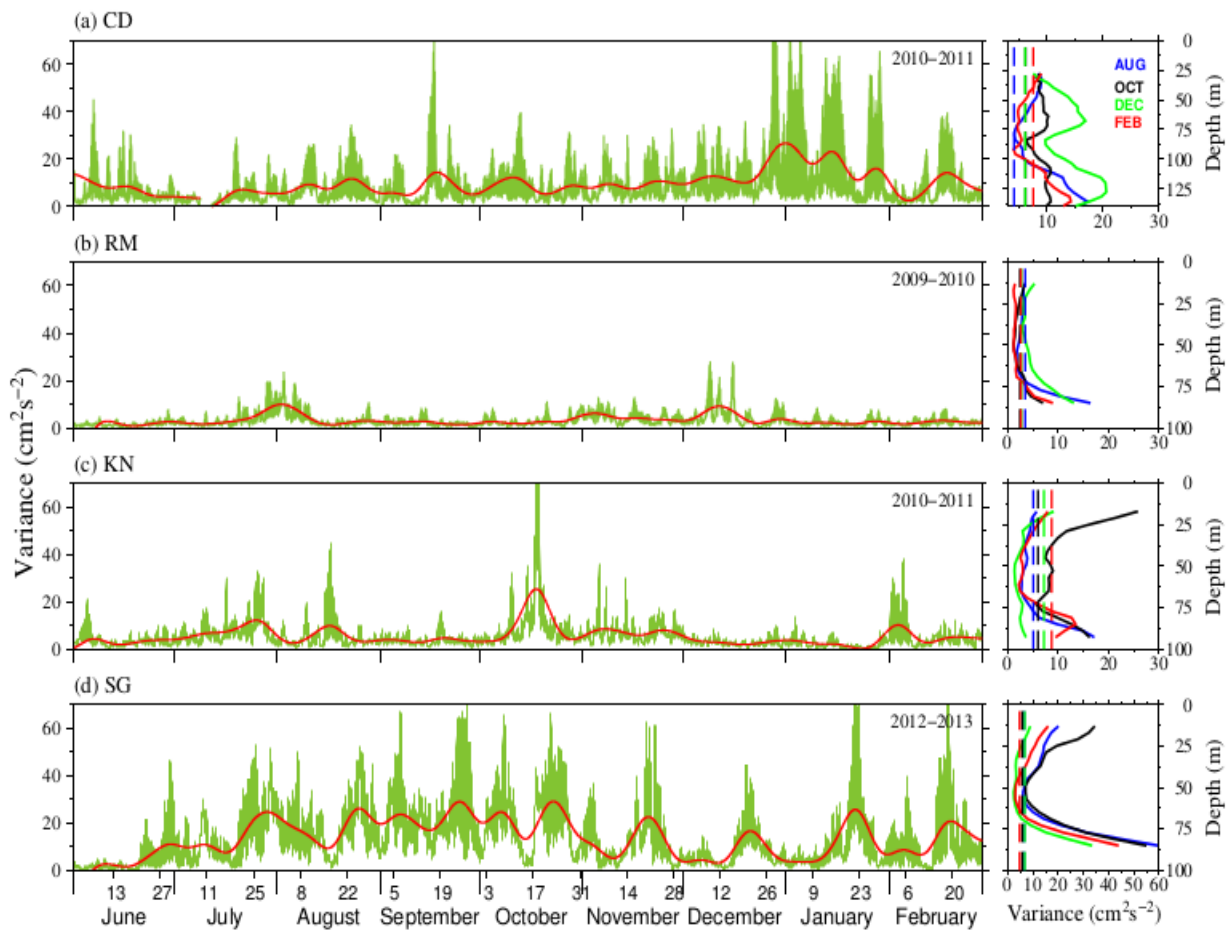


Fig. 10: Criticality (γ/c) computed from the slope of internal wave characteristics (using climatology of temperature and salinity) and topographic slope (using SRTM30_plus bathymetric data) near to the ADCP moorings. Black star represents the location of ADCP mooring on the shelf. Buoyancy frequency at upper 250m in August (green), October (red) and December (black) computed from climatology are also shown. The circles represents the values of buoyancy frequency computed using temperature and salinity profiles available near to the ADCP moorings and the location of the profiles is given in the 2D plot with circles in same the colour. Period of observation each profiles is shown in the figure.

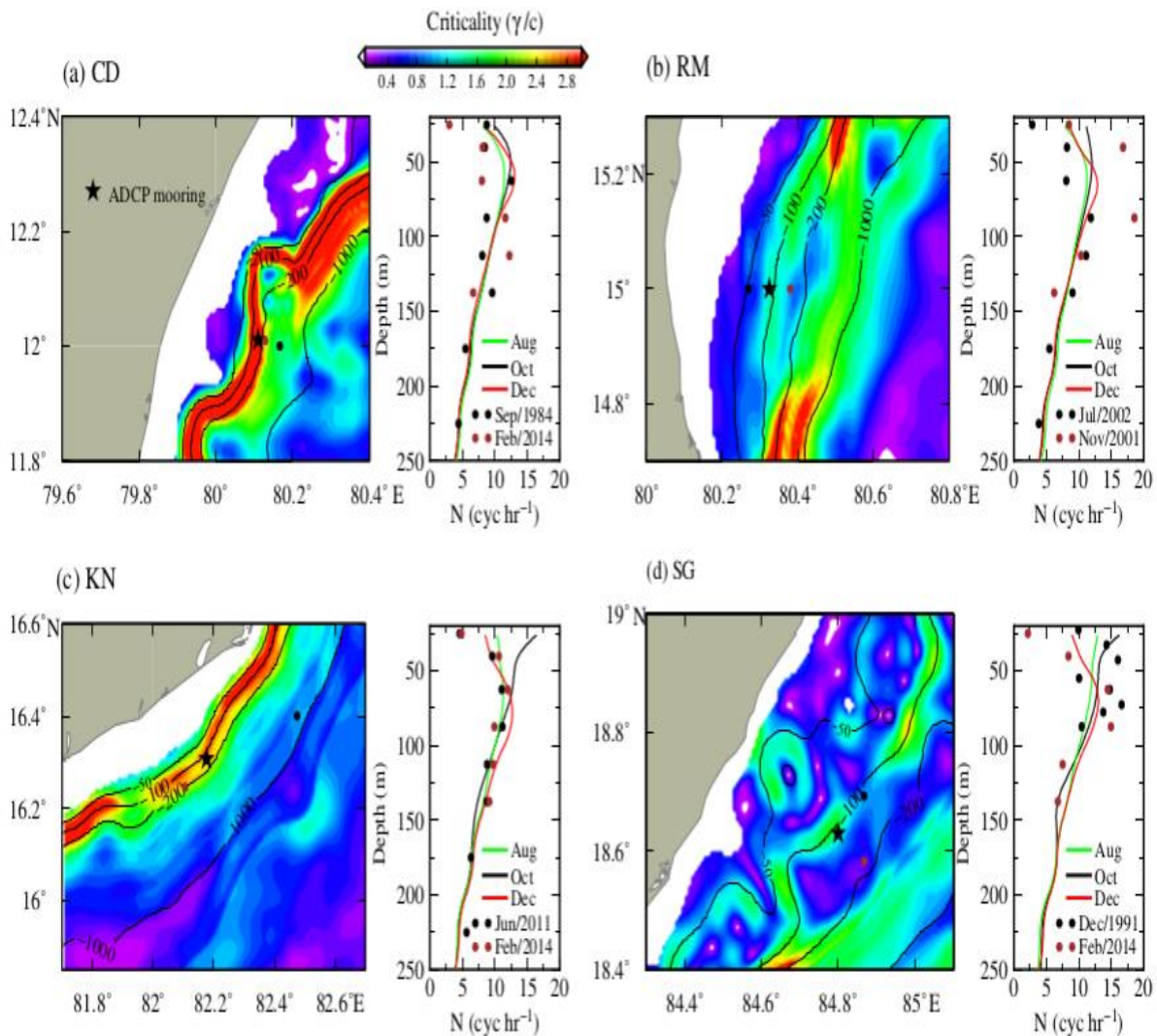


Fig. 11: Results of CEOF analysis of semidiurnal internal tides for a 9-month period on the shelf off (a) CD, (b) RM, (c) KN and (d) SG. First three modes are shown. Amplitude, phase and percentage of variance for each EOF mode for both cross-isobath and along-isobath component of semidiurnal internal tides. First three EOF modes are shown in red, blue and black lines respectively.

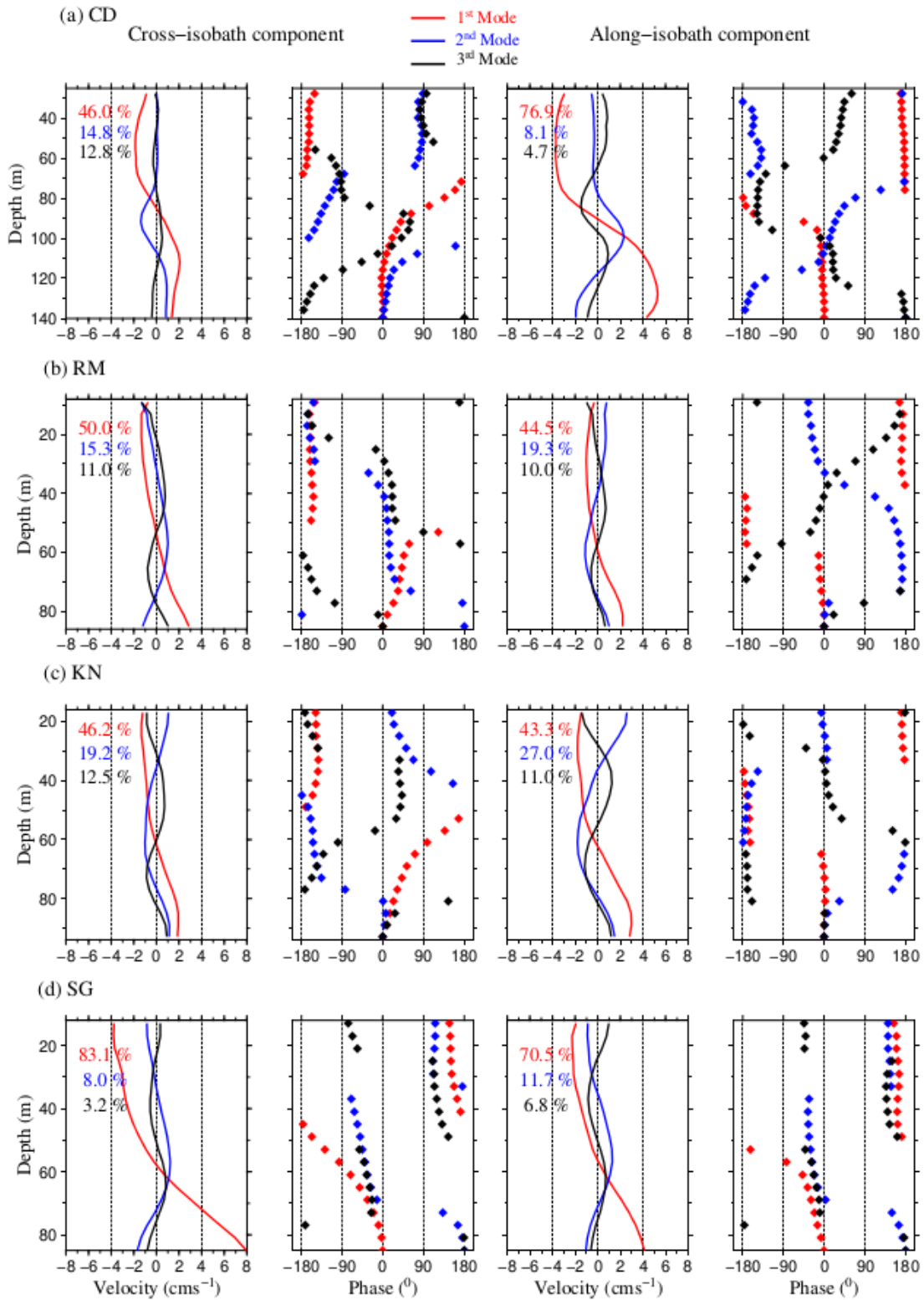
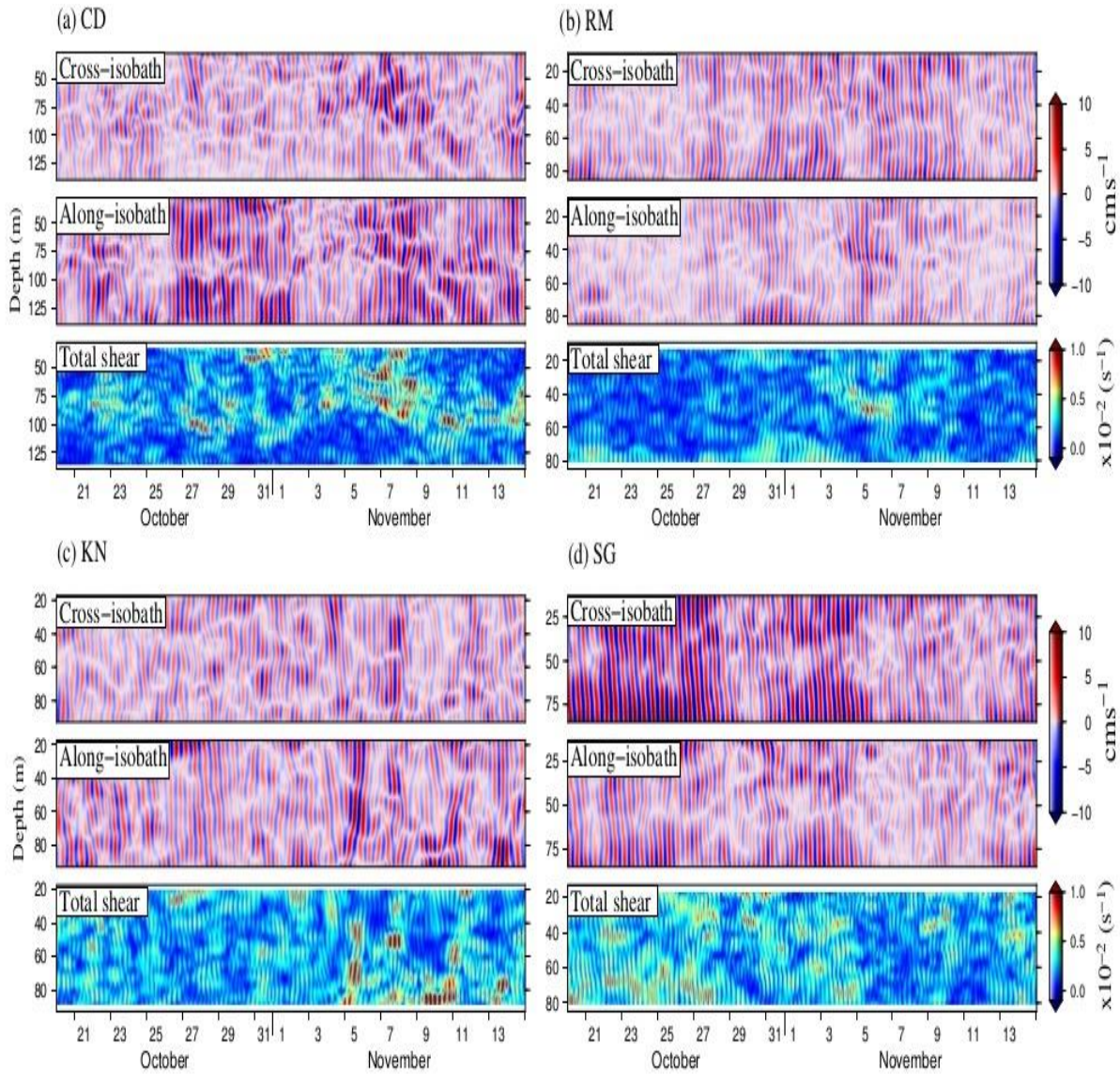


Fig. 12: Time series of cross-isobath (first panel) and along-isobath (second panel) component of semidiurnal internal tides and total semidiurnal vertical shear (third panel) for a 20-day period on the shelf off (a) CD, (b) RM, (c) KN and (d) SG.



Tables

Table 1: Amplitude and phase of major tidal constituents from Admiralty Tide Tables (ATT) along the east coast of India. Phase (g^0) is with respect to local time (GMT + 5.5 hours) and unit is in degrees.

Constituents	Chennai (11^0 N)		Vishakhapatnam (17.6^0 N)		Paradip (20.3^0 N)	
	Amp (cm)	Phase (g^0)	Amp (cm)	Phase (g^0)	Amp (cm)	Phase (g^0)
M2	33.2	237.3	47.5	239.0	62.2	241.4
S2	13.7	272.6	20.9	274.2	27.9	276.9
N2	07.2	228.7	10.1	231.0	13.1	228.9
K1	09.0	338.0	11.3	336.4	12.4	330.8
O1	02.8	310.1	04.1	320.5	04.9	320.2

Table 2: Details of ADCP moorings on the shelf off the east coast of India and period of current observation. Angle of rotation is the local bathymetric angle which is used to calculate the cross-isobath and along isobath component of tidal currents.

Mooring Location	Lon/ Lat ($^{\circ}$ E / $^{\circ}$ N)	ADCP Depth (m)	Water Depth (m)	Sampling Interval Time/vertical	Angle of rotation	Shelf width (km)	Period of Observation	
							Start date	End date
Cuddalore (CD)	80.100 / 12.010	140	150	15 min / 4 m	-15.76 $^{\circ}$	40	01-05-2010	24-03-2011
Ramayapatnam (RM)	80.336 / 15.00	92	100	30 min / 4 m	00.00 $^{\circ}$	60	19-04-2009	28-04-2010
Kakinada (KN)	82.170 / 16.30	95	120	15 min / 4 m	-55.07 $^{\circ}$	30	13-05-2010	27-03-2011
South of Gopalpur (SG)	84.788 / 18.646	90	97	15 min / 4 m	-50.76 $^{\circ}$	55	16-02-2012	10-03-2013

Table 3: Barotropic ellipse parameters of major semidiurnal constituents with 95% confidence interval on the ADCP locations obtained by harmonic analysis of 9-month long data using t_tide tool are shown. Negative value of semiminor axis indicates that the ellipses are traversed in clockwise direction. Phase (g) is with respect to local time (GMT + 5.5 hours) and unit is in degrees.

Locations		Semimajor axis (cms^{-1})	Semiminor axis (cms^{-1})	Inclination ($^{\circ}$)	Phase g ($^{\circ}$)	Signal-noise ratio
CD						
	M ₂	1.87±1.01	0.49±0.69	119.09±23.53	154.13 ± 27.63	3.5
	S ₂	1.63±0.92	0.21±0.49	89.52±19.23	165.00 ±33.28	3.1
RM						
	M ₂	2.61± 0.39	-1.02±0.50	142.15±10.17	160.82± 09.11	45.0
	S ₂	1.21±0.32	-0.43±0.41	156.24±29.60	213.20 ± 20.17	14.0
KN						
	M ₂	3.47± 1.18	0.19±1.12	53.92±16.80	172.39 ±19.60	9.6
	S ₂	1.51±0.91	-0.07±1.04	51.95 ±43.93	154.87±43.18	2.8
SG						
	M ₂	3.98±0.57	-1.11± 0.81	82.33±11.22	162.47± 8.85	49.0
	S ₂	1.90±0.57	-0.45± 0.78	101.70±23.03	185.99±20.16	11.0

Table 4: Percentage of variance explained by running harmonic analysis in the total semidiurnal band on the shelf in different time windows.

Window used for Harmonic analysis	CD %	RM %	KN %	SG %
3 day	93	92	91	95
7day	79	70	68	88
15 day	64	52	43	78
30 day	43	34	28	64
60 day	19	21	17	37
Full period (9 month)	6	5	2	8

Appendix A: Baroclinic ellipse parameters for M_2 , S_2 , N_2 and K_1 for July-August, September-October, November-December and January-February at various depths on the shelf are presented.

Locations	Constituent	Depth (m)	Semimajor/semiminor axis (cms^{-1})			
			Jul-Aug	Sep-Oct	Nov-Dec	Jan-Feb
CD	M2	32	2.39/0.16	3.61/-0.72	1.07/-0.12	3.70/0.21
		80	2.23/0.03	1.16/-0.60	2.93/-1.22	2.64/-1.18
		140	4.36/-0.52	3.27/-1.62	4.08/-1.92	4.33/-0.93
	S2	32	2.48/-0.42	1.73/0.45	2.35/0.52	1.66/0.20
		80	1.17/0.31	1.13/-0.24	1.76/-0.46	1.42/0.30
		140	3.48/-0.56	2.05/0.77	2.53/-0.82	2.52/-0.52
	N2	32	2.49/-0.40	0.58/-0.05	0.99/0.06	2.07/0.10
		80	1.26/-0.35	1.74/0.34	1.46/-0.01	2.06/-0.63
		140	3.56/-0.53	2.18/-0.71	2.15/-0.08	4.27/-0.60
	K1	32	0.99/0.46	1.22/-0.41	2.73/-0.30	1.17/0.38
		80	1.43/0.30	1.66/0.24	1.51/-0.21	0.79/-0.02
		140	0.98/-0.04	0.71/0.40	1.59/-0.19	1.53/-0.72
RM	M2	13	0.83/-0.62	0.61/-0.04	2.81/-0.32	1.07/-0.39
		53	0.61/-0.06	1.01/0.05	0.62/-0.38	0.43/-0.16
		85	1.83/-1.22	0.83/0.47	5.68/0.59	1.44/-0.95
	S2	13	1.14/-0.21	1.46/-0.07	0.45/0.08	0.24/-0.05
		53	0.73/-0.01	0.85/-0.48	0.66/0.01	0.34/-0.01
		85	3.15/-1.35	2.28/-0.44	0.50/0.13	1.95/-0.77
	N2	13	0.71/-0.44	0.47/-0.02	2.19/-0.13	0.31/0.06
		53	0.41/-0.02	0.43/-0.01	0.49/-0.29	0.25/-0.10
		85	0.26/0.10	1.12/-0.49	3.46/-0.46	0.59/-0.36
	K1	13	2.19/-1.71	1.29/-1.21	2.72/-0.97	1.60/-1.15
		53	0.80/-0.55	0.80/-0.64	1.45/-0.39	0.48/-0.10
		85	0.87/-0.44	1.19/-0.53	1.99/-0.51	1.57/-0.52
KN	M2	17	2.50/-1.3	1.45/-0.03	2.19/0.63	1.92/-1.36
		57	1.05/0.04	1.34/-0.54	1.38/-0.01	0.61/0.17
		93	3.95/0.26	1.95/0.62	0.65/0.04	1.54/-0.07
	S2	17	1.65/0.02	3.22/-0.56	2.05/0.50	1.70/-0.16
		57	0.98/-0.28	0.50/-0.47	1.60/0.16	0.37/-0.07
		93	3.47/-0.29	0.60/0.42	1.49/0.82	1.84/0.30
	N2	17	2.03/-0.46	0.71/-0.22	2.19/-0.36	1.57/0.60
		57	0.42/-0.34	1.58/0.04	0.66/0.07	0.73/-0.22
		93	1.91/-0.48	3.48/0.46	1.07/0.40	3.05/0.36
	K1	17	2.27/-1.37	1.01/-0.38	2.53/-0.20	1.69/-1.06
		57	1.67/-0.31	0.55/0.01	1.63/-0.01	0.46/-0.01
		93	2.35/-0.57	1.77/-0.14	2.48/-1.43	0.97/-0.64
SG	M2	13	6.67/-2.53	7.47/-3.89	3.35/-0.8	6.28/-2.44
		49	2.49/0.13	3.61/-1.64	1.25/-0.57	2.43/-0.72
		85	10.67/-5.83	12.68/-6.93	7.70/-3.23	13.36/4.67
	S2	13	2.75/-1.46	4.54/-2.27	1.83/-1.38	2.25/-0.89
		49	1.59/-0.20	2.24/-1.25	0.59/-0.20	1.41/-0.12

	85	6.79/-2.69	8.47/-3.55	2.71/-0.69	5.70/-1.96
N2	13	2.58/-0.23	1.22/0.38	3.40/-0.12	3.34/-0.83
	49	1.96/-0.76	0.74/0.32	1.05/-0.80	0.77/0.26
	85	5.04/-4.12	3.15/0.24	5.44/-2.44	3.87/-0.60
K1	13	1.49/-1.26	1.39/-0.83	3.09/-1.16	3.77/-2.93
	49	0.95/-0.85	0.62/-0.29	1.06/0.15	0.64/-0.20
	85	1.08/-0.15	1.51/-0.34	1.40/-1.15	1.58/-0.04
